Applied Ocean Research 161 (2025) 104692

Contents lists available at ScienceDirect

Applied Ocean Research

journal homepage: www.elsevier.com/locate/apor

High speed planing craft dynamics in irregular waves: Safety improvement using interceptor systems

Fatemeh Roshan [a,*], Rasul Niazmand Bilandi [a,b], Fabio De Luca [c], Simone Mancini [c], Pentti Kujala [a], Abbas Dashtimanesh [d]

[a] Estonian Maritime Academy, Tallinn University of Technology, Tallinn, Estonia
[b] Department of Aero and Hydrodynamics, Force Technology, Kgs. Lyngby, Denmark
[c] Department of Industrial Engineering, University of Naples "Federico II," Naples, Italy
[d] Engineering Mechanics Department, School of Engineering Science, KTH Royal Institute of Technology, 100 44 Stockholm, Sweden

ARTICLE INFO

Keywords:
High speed planing craft
Irregular head waves
Human safety
Interceptor
Double interceptor system

ABSTRACT

This study investigates the potential for improving the dynamic performance and human safety of High-Speed Planing Craft (HSPC) in irregular head waves through the implementation of a Transom Interceptor System (TIS) and a Double Interceptor System (DIS). Experimental tests measure hull resistance, heave and pitch motions, and vertical accelerations in semi-planing, transient, and planing modes. The recorded data for the bare hull, the hull equipped with TIS in transient mode, and the hull equipped with TIS and DIS in planing mode are compared to evaluate the interceptor performance in improving the dynamics of HSPC. Additionally, the crew safety exposed to vertical acceleration is evaluated according to the ISO 2631–1 (1997), ISO 2631–5 (2004), and EU Directive 2002/44/EC (2002). The results indicate that TIS effectively enhances dynamic performance in transient and planing modes as well as human safety and comfort by reducing moderate vertical acceleration. However, in transient mode, TIS may amplify impact shocks, increasing the possibility of adverse health effects. Moreover, the DIS increases hull motions, vertical acceleration, and the potential for health and comfort risks in planing mode. These findings emphasize the potential of TIS in enhancing HSPC dynamics and safety, while it is crucial to optimize interceptor configurations based on operational speeds.

1. Introduction

High-speed planing craft (HSPC) are commonly used in various maritime missions that demand high-speed operations, such as patrol, racing, and search and rescue. However, the performance of HSPC in rough waters is significantly influenced by the hull's dynamic behavior and crew's safety.

Operating at high speeds in rough waters exposes HSPCs to severe hull motions and harsh accelerations, as demonstrated by Roshan et al. (2022) and Niazmand Bilandi et al. (2024). These conditions can lead to increased structural stress, compromised hull stability and control, and safety risks for crews exposed to such accelerations. The effect of vertical accelerations on human health and comfort aboard high-speed craft has been analyzed by Allen et al. (2008), Dobbins et al., (2008), Garme et al. (2011), and Taunton et al. (2011), indicating a high possibility of safety risks for onboard crews.

While reducing hull speed on rough water can effectively minimize hull motions and accelerations and consequently reduce the probability of adverse health risks for the crews, it contradicts the primary purpose of HSPCs, particularly in time-critical missions such as rescue operations. As a result, improving HSPC performance necessitates the implementation of shock/vibration mitigation devices to reduce the transfer of hull accelerations to the human body, as well as motion reduction devices to prevent severe accelerations in rough seas (Roshan et al., 2024).

Although both strategies improve human safety onboard the HSPC, motion reduction devices offer additional advantages. These devices not only reduce the risk of adverse health effects caused by hull accelerations but also improve hull stability and control (Lau et al., 2024; Niazmand Bilandi, 2024). These are useful to reduce the likelihood of critical events such as loss of stability, impaired maneuverability, or even hull capsizing under challenging wave conditions by minimizing excessive motions. This improvement underscores the importance of implementing advanced motion-control devices to ensure both safety and dynamic performance.

* Corresponding author.
E-mail address: fatemeh.roshan@taltech.ee (F. Roshan).

https://doi.org/10.1016/j.apor.2025.104692
Received 12 February 2025; Received in revised form 27 May 2025; Accepted 30 June 2025
Available online 7 July 2025

Nomenclature and observations

A_{iz} i^{th}	peak of acceleration between two zero crossings
$a_{1/n}$	Mean of 1/n highest height of vertical acceleration
$a_w(t)$	Frequency-weighted acceleration signals (ms^{-2})
B_{WL}	Maximum moulded breadth at water line (m)
F_p	Peak frequency
Fr_B	Beam Froude number
g	Acceleration of gravity (ms-2)
CG	Centre of Gravity
$H_{1/n}$	Mean of 1/n highest height of heave motion
H_s	Significant wave height (m)
K	Wave number (m^{-1}), ω^2/g
K_{xx}	Roll radius of gyration (m)
K_{yy}	Pitch radius of gyration (m)
L_{CG}	Longitudinal center of gravity (m)
L_{OA}	Overall length of the hull
L_{WL}	Length of waterline (m)
m	Applied mas (kg)
R_w	Total resistance of model in waves (kg)
S	Wave steepness (radian), $K.H_s/2$.
T	Measurement time (s)
t_d	Duration of the daily exposure
T_p	Peak period (s)
V_{CG}	Vertical center of gravity (m)
x	Distance from the center screw (m)
β_T	Deadrise angle at the transom (deg)
$\beta_{0.5}$	Deadrise angle at 0.5 L_{WL} (deg)
$\beta_{0.75}$	Deadrise angle at 0.75 L_{WL} (deg)
γ	Overshoot Parameter
Δ	Displacement (buoyant) force (kg)
θ	Pitch or trim angle (deg)
$\theta_{1/n}$	Mean of 1/n highest height of pitch motion (deg)
λ	Wavelength (m)
ω	Angular Frequency ($radians^{-1}$), $\omega = 2\pi F_p$
CF	Crest Factor
DII	Dipartimento di Ingegneria Industriale
DIS	Double Interceptor System
HSPC	High Speed Planing Craft
ISO	International Standard Organization
NSS	Naples Systematic Series
PSD	Power Spectral Density
RMS	Root Mean Square of weighted frequency acceleration (ms^{-2})
SF	Scale Factor
TIS	Transom Interceptor System
VDV	Vibration Doze Value (ms^{-2})
WBV	Whole Body Vibration

There are numerous documents indicating that using a Transom Interceptor System (TIS) can efficiently reduce hull resistance and trim angle in calm water, such as John et al., (2011), Day and Cooper (2011), Karimi et al. (2013), and Seok et al. (2020). Furthermore, Najafi et al. (2015), Karimi et al. (2015), and Suneela and Sahoo (2021) highlighted the effectiveness of TIS in reducing vertical motions and accelerations in regular waves. However, despite these valuable insights, most existing research focuses on calm water or regular wave conditions, which do not fully represent the complex and random nature of real sea states. Therefore, the TIS performance in irregular wave conditions remains relatively limited, particularly regarding its influence on human safety.

Assessment of human safety affected by HSPC acceleration requires statistical analysis under irregular waves due to their random characteristics, as regular wave tests lack this complexity and cannot be statistically analyzed in accordance with safety standards (ISO 2631 or EU Directives). However, there is a significant knowledge gap concerning the effects of TIS in irregular wave conditions, which are critical for human safety assessments.

In addition to the conventional transom interceptor, De Luca and Pensa (2011) introduced an unconventional interceptor configuration consisting of a TIS and an additional interceptor located in the middle of hull length. This Double Interceptor System (DIS) is an innovative configuration designed to generate an extra lift force at the forward interceptor position, potentially leading to more reduction in hull motions. Furthermore, DIS can generate an air cavity behind the forward interceptor, which contributes to a reduction in hull shear resistance. The performance of DIS in calm water and regular waves has been presented in De Luca and Pensa (2012). They observed the possibility of increasing hull motions and accelerations when using DIS in regular waves, though it is efficient in resistance reduction. However, the dynamic performance of a hull equipped with DIS in irregular waves remains unexplored, highlighting a gap that must be addressed for a comprehensive understanding of DIS behavior.

Although interceptors are designed to reduce hull motions and resistance, their performance can significantly vary depending on the hull's operational speeds. For instance, Tsai and Hwang, (2004), Mansoori and Fernandes (2017), and Suneela et al. (2020) demonstrate the possibility of negative trim angles (bow down) in planing mode when an improperly designed interceptor is employed. However, these studies also highlight that such an interceptor can be effective in correcting trim angle and reducing hull resistance at lower speeds. This variability underscores the importance of designing interceptors that are optimized for the intended operational speed range for the hull. An interceptor optimized for lower speeds might become unsuitable at higher speeds, potentially leading to stability issues and compromising overall performance.

In addition to the importance of selecting an appropriately designed interceptor for an HSPC to minimize hull motions and resistance at operational speeds, it is also crucial to consider the impact of interceptors on motion accelerations. This aspect directly affects human safety onboard the HSPCs, as severe accelerations can cause discomfort, fatigue, and impaired the crew performance and their ability to carry out duties, and adverse health effects. Therefore, designing an appropriate interceptor must prioritize both dynamic efficiency and reducing vertical acceleration to enhance human safety.

This study aims to investigate the potential for improving the dynamic behaviors of HSPCs and crews' safety in irregular head seas by employing different configurations of interceptors tailored to operational speeds. To achieve this, the objectives include:

- Improving HSPC seakeeping and the crew's safety onboard in transient mode using TIS.
- Improving HSPC seakeeping and the crew's safety onboard in planing mode using TIS and DIS.

By addressing these objectives, this study seeks to provide valuable insights into the potential for improving both the dynamic performance of HSPCs and human safety under realistic sea conditions by employing an interceptor system.

For this purpose, a high-speed planing hull, model C5, is tested in a towing tank under three different irregular wave conditions at various speeds, representing semi-planing, transient, and planing modes. Subsequently, different interceptor configurations are installed on the hull, and the tests are repeated for the hull equipped with interceptors. The obtained results for the dynamic behaviors and human safety of the hull equipped with interceptors are compared to those of the bare hull. This

comparative analysis aimed to evaluate the efficiency of each interceptor configuration in improving the seakeeping performance and human safety of an HSPC.

The remaining part of this study is structured as follows: after the introduction, Section 2 presents the experimental procedure for measuring hull motions and accelerations in irregular waves, model characteristics, and the properties of considered wave conditions. Section 3 discusses the measures used for evaluating human safety based on current safety standards for humans exposed to WBVs and shocks. In Section 4, the results are presented, which include the data representation method (Section 4.1) and an investigation of the dynamic behaviors of the bare hull, the hull with TIS in transient mode, and the hull with TIS and DIS in planing mode (Section 4.2). Additionally, Section 4.3 predicts the possibility of adverse health effects and discomfort for the bare hull, examines safety improvements using TIS in transient mode, and explores safety improvement in planing mode using TIS and DIS. Finally, discussion and conclusions are provided in Sections 5 and 6, respectively.

2. Experimental procedures

The towing tank tests for this study is carried out at the Department of Industrial Engineering (DII) of the Università degli Studi di Napoli "Federico II". The towing tank facility has a length of 136.0 m, a width of 9.0 m, and a depth of 4.5 m. The carriage has a maximum speed of 10.0 ms^{-1}. For this study, tests are performed at speeds of 2.5, 3.5, 4.5, and 6.0 ms^{-1}, corresponding to the beam Froude numbers of 1.2, 1.7, 2.2, and 3.0. These Froude numbers are chosen to represent semi-planing, transient, and planing modes for an HSPC.

A hard-chine hull model from the Naples Systematic Series (NSS), as published in De Luca and Pensa (2019), are tested with and without the interceptor system. Fig. 1 shows the hull model C5 from NSS, and the details of model geometry are provided in Table 1.

During the experiments, two interceptors are added to the hull: a transom interceptor with a height of 2 mm and a length of either 0.5 B_{WL} or 0.25B_{WL} (as explained in Section 4, Results), and a forward interceptor with a height of 2 mm and a length equal to the full B_{WL}, located 0.8 m forward of the transom.

The vertical and longitudinal positions of the model's center of gravity were determined using an inertial balance equipped with a longitudinal weight rack (As shown in Fig. 2). After weighing the bare hull with all instrumentation installed, the model was placed on the balance, and its L_{CG} was found by translating it along the platform until a horizontal equilibrium was achieved, at which point the pivot point of the balance coincided with the L_{CG}. The V_{CG} was then determined by applying a known mass m at a known distance x from the central axis of

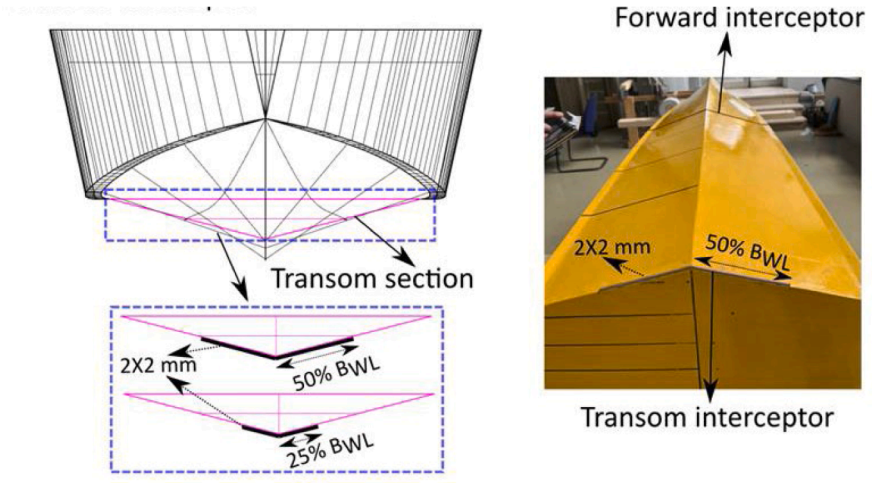

(a)

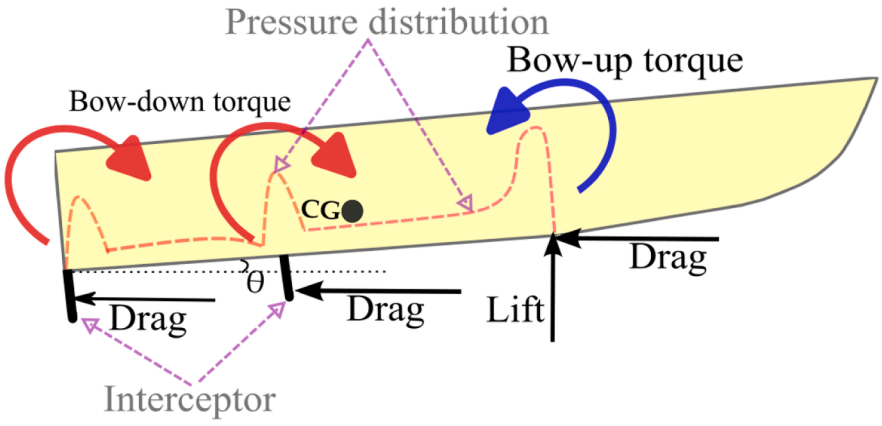

(b)

Fig. 1. HSPC hull (model C5 of NSS) and b) A schematic of hull with DIS.

Table 1
Hull characteristics for model C5.

Parameter	Value
L_{OA} (m)	2.611
L_{WL} (m)	2.400
B_{WL} (m)	0.41
L_{CG} (m)	0.945
V_{CG} (m)	0.205
SF	15
Δ (kg)	37.4
Kxx/B_{WL}	0.4
Kyy/L_{wl}	0.25
β_T (deg)	13.2
$\beta_{0.5}$ (deg)	22.3
$\beta_{0.75}$ (deg)	38.5

the weight rack and measuring the resulting trim angle θ. Using multiple combinations of m and x, the V_{CG} was calculated from the relation.

$$V_{CG} = \frac{mx\cot(\theta)}{m+M} \quad (1)$$

where M is the hull mass. To determine the radii of gyration, the hull was suspended at the pivot point and subjected to free oscillations in both roll and pitch. The resulting motions were recorded using accelerometers, from which natural frequencies and oscillation angles were extracted. These measurements were used to calculate the radii of gyration in roll (K_{xx}) and pitch (K_{YY}).

The natural periods of oscillation were recorded using a stopwatch and repeated five times to ensure consistency. The average values were then used to calculate the radii of gyration using the standard pendulum formula. The total mass of the model was measured using an electronic scale with 0.01 kg accuracy. All mass properties were determined before towing tests and remained unchanged throughout the experiments.

During the towing tank test, two triaxial accelerometers are used to record the hull acceleration at CG and at 0.5 L_{WL} forward from the CG. These accelerometers are Cross Bow CXL04GP3-R-AL, with an input range (g) of ±4, noise (mgrms) of 10, and bandwidth (Hz) of DC-100, with a sensitivity (mV/g) of 500 ± 15. Additionally, hull resistance is measured by an HBM load cell (PW115AH 20 kg, accuracy Class III), suitable for applications requiring reliable accuracy.

The dynamic performance of hull model C5 is tested by allowing free heave and pitch motions while the model is restrained in the surge direction by the towing carriage. Furthermore, a Qualisys Motion Capture System is used to measure hull motions in wave conditions. This is a high-precision optical tracking system that is widely used in engineering applications.

The model's dynamic behavior is studied in three different irregular head waves from the JONSWAP spectrum, as presented in Table 2. The produced wave profile with towing tank wave makers is verified by employing two ACAMINA AWP-24–2 Wave Height Gauges sensors (a capacitive probe that is used for measuring wave height in the towing tank) fixed on the towing tank and four Baumer UNDK 30U6103 sensors (an ultrasonic proximity sensor designed to measure distances with high precision and reliability) fixed on the carriage are employed.

To ensure a reliable comparison between the results for the bare hull and the hull equipped with the interceptor system, it is crucial to analyze the hull behavior in the same wave spectra. Therefore, recorded wave heights by capacitive probes are measured and compared with theoretical spectra to verify the generated wave spectrum. Fig. 3 shows the comparison of generated wave spectra with theoretical JONSWAP spectra.

Furthermore, the recorded data are sampled at a frequency of 500 Hz and filtered with a Butterworth bandpass filter of 0.05–20 Hz. To analyze the recorded data for unsteady phenomena, a large number of tests are required to ensure the reliability of the statistical approaches. Therefore, several tests (15 or more) are carried out to reach a sufficient number of wave encounters (about 200). In this regard, 256 (2^8) Fourier components are used. The repetition period is 250 s, a single random seed is generated to build the wave profile in the time domain, and the start time of wave generation is shifted from run to run.

3. International standards for evaluating acceleration exposure

For a high-speed planing craft operating in rough water, hull acceleration can affect human safety. Exposure to this acceleration may cause adverse health effects, discomfort, and motion sickness for the occupants.

There are various standards and regulations that investigate the safety of humans exposed to WBV and shocks in a vibrated environment.

Table 2
Characteristics of considered irregular head waves.

Wave condition	Spectrum	H_s (m)	$H_{s\text{-}full\text{-}scaled}$ (m)	γ	T_p (s)	$T_{p\text{-}full\text{-}scaled}$ (s)	F_p(Hz)
1	JONSWAP	0.075	1.125	3.3	1.52	5.89	0.66
2	JONSWAP	0.060	0.9	3.3	1.356	5.25	0.737
3	JONSWAP	0.045	0.675	3.3	1.176	4.55	0.850

Fig. 2. Determining the CG position and radii of gyration for model C5.

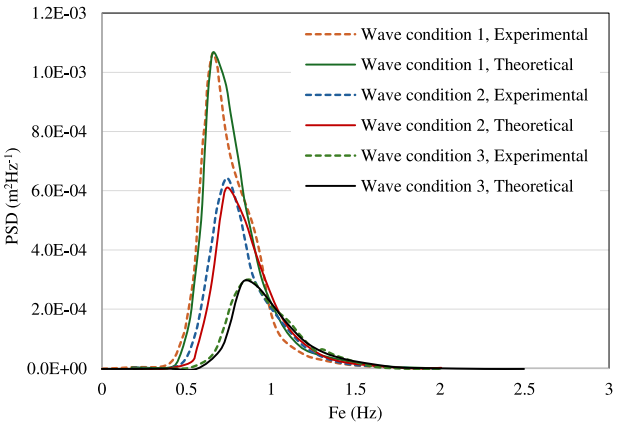

Fig. 3. Generated wave spectra and theoretical JONSWAP wave spectra.

This study uses ISO 2631-1, (1997); ISO 2631-5, (2004), , and Directive 2002/44/EC, (2002) to assess the health and comfort risks onboard the HSPC in different wave conditions and speeds. Additionally, the effectiveness of using an interceptor system in improving the safety of HSPC crews is examined using these standards.

For this purpose, vertical accelerations measured in the CG and bow during the towing tests are used to calculate the root mean square (RMS) and vibration dose value (VDV). These parameters are recognized by the standards as measures for assessing the effects of WBV and shock exposure on human health and comfort as

$$RMS = \left\{ \frac{1}{T} \int_0^T a_w^2(t)dt \right\}^{1/2} \tag{2}$$

$$VDV = \left\{ \int_0^T [a_w(t)]^4 dt \right\}^{\frac{1}{4}} \tag{3}$$

where *RMS* represents the root mean square of frequency-weighted acceleration, $a_w(t)$ is the frequency-weighted acceleration signal, and T is the measurement time for acceleration exposure, which is computed based on Eq. (4) for the full-scale boat.

$$T = T_{\text{model}}\ SF^{0.5} \tag{4}$$

Frequency-weighted accelerations are calculated by transferring recorded acceleration to the frequency domain and multiplying the data by the weighting transfer function recommended by ISO 2631-1, (1997). Afterward, the frequency-weighted accelerations are transformed back to the time domain. Fig. 5 shows a sample of frequency-weighted acceleration compared to the unweighted signals in wave condition 1 at $Fr_B = 2.2$. In this Figure, the real-time duration of the experiment is 207.18 s, which has been scaled to 802.41 s for the full-scale hull using Eq. (4).

ISO 2631-1, (1997) considers the RMS value as a key parameter to predict human discomfort due to WBVs and shocks. According to this standard, an RMS value below 0.315 ms^{-2} is considered to represent a "not uncomfortable" level, while values between 0.315 and 0.63 ms^{-2} are associated with "a little discomfort". As the RMS increases, the likelihood of discomfort rises. Specifically, RMS values between 0.5 and 1 ms^{-2} indicate "fairly uncomfortable," values between 0.8 and 1.6 ms^{-2} suggest "uncomfortable," and values between 1.25 and 2.5 ms^{-2} denote a "very uncomfortable" condition. Additionally, ISO 2631-1, (1997) defines an RMS value above 2 ms^{-2} as indicating an "extremely uncomfortable" condition. Fig. 4

The RMS value is also used by ISO 2631-1, (1997) to assess the possibility of adverse health effects as a result of accelerations. However, predicting the probability of health risks in EU Directive 2002/44/EC, (2002) estimates considers the VDV value. This study follows the EU Directive 2002/44/EC, (2002) guidance for evaluating the effects of HSPC acceleration on human health since VDV is the fourth power of accelerations and is more sensitive to the acceleration peak. For a high-speed planing craft operating in rough water, impact shocks could be so harsh with a serious effect on human health, while RMS value might underestimate the effects of these shocks.

EU Directive 2002/44/EC, (2002) considers VDV_{8h} to predict the possibility of adverse health effects during the 8-hour work shift. VDV_{8h} are computed as:

$$VDV(8h) = VDV.\left[\frac{t_d}{T}\right]^{1/4} \tag{5}$$

where t_d is the duration of the daily exposure, which is 8 h here. Directive 2002/44/EC, (2002) introduces 9.1 $ms^{-1.75}$< VDV_{8h} as the action value that requires reducing WBVs and shocks to avoid health problems. Additionally, there is a high probability of health negative effects that requires immediate action to prevent health risks if VDV_{8h} becomes higher than the limit value (21.0 $ms^{-1.75}$ < VDV_{8h}).

According to ISO 2631-5, (2004), long-term whole-body multiple shocks can lead to adverse health effects, particularly affecting the lower lumbar spine and connected nervous system. The relationship between the input vertical shock and the peak acceleration response in the spine is described by Eq. (6) for an 8-hour daily work shift.

$$S_{ed} = \left[(m_k D_{zd})^6\right]^{1/6} \tag{6}$$

where, m_z=*0.032* MPa/ms^{-2} is defined by ISO 2631-5, (2004), and D_{zd} is computed as,

$$D_{zd} = D_z\left[\frac{t_d}{T}\right]^{1/6} \tag{7}$$

D_z in Eq. (6) is the average daily dose in the vertical direction defined as

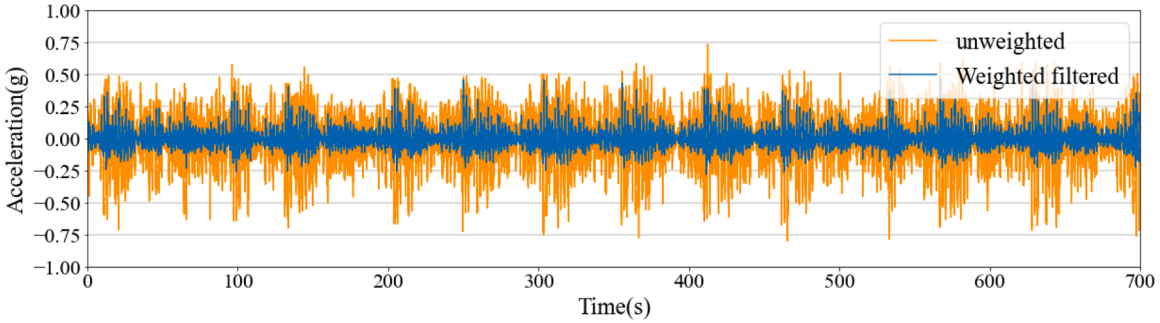

Fig. 4. Weighted filtered acceleration and unweighted acceleration of bare hull at $Fr_B = 2.2$.

$$D_z = \left[\sum_i A_{iz}^6\right]^{1/6} \quad (8)$$

where A_{iz} is the i^{th} peak of the response acceleration between two zero crossings. It should be noted that counting peak accelerations in vertical direction only contains positive peaks.

According to ISO 2631-5, (2004), $S_{ed} < 0.5$ MPa indicates a low probability of adverse health effects, whereas 0.8 MPa $< S_{ed}$ indicates a high probability of negative health effects. These values are considered for 220 workdays during a year, for a person who started being exposed at the age of 20 to 65 years.

By considering these standards, a comparison of the RMS, VDV_{8h}, and S_{ed} values for the bare hull and the hull equipped with an interceptor system can be used to examine the effectiveness of the interceptor system in improving human safety onboard an HSPC.

4. Results

The following subsections first examine the dynamic characteristics of the bare hull, the effects of a transom interceptor system (TIS) in transient mode, and the effects of the TIS and double interceptor system (DIS), individually, in planing mode. These analyses provide insights into resistance, heave and pitch motions, and vertical acceleration at the CG and bow. Subsequently, human safety factors are assessed based on ISO 2631-1, (1997); ISO 2631-5, (2004) and EU Directive 2002/44/EC, (2002), with a focus on the potential for reducing adverse health risks and discomfort achieved through the TIS in transient mode, TIS in planing mode, and DIS in planing mode.

There are three different configurations suggested for the interceptor system in this study. The first recommended configuration for the transient mode ($1.7 < Fr_B < 2.2$) consists of a transom interceptor with a height of 2 mm and a length of $0.5B_{WL}$. A comparison between the results for the bare hull and the hull equipped with this TIS demonstrates the effectiveness of using the TIS to improve the dynamic performance of HSPC and human safety in transient mode.

In planing mode ($Fr_B = 3$), a double interceptor system (DIS) is implemented on the hull bottom. This system consists of a transom interceptor and another interceptor located at the middle of the hull length. Both interceptors are designed with a height of 2 mm, and an initial length of $0.5B_{WL}$ for the transom interceptor, and a length of B_{WL} for the forward interceptor. However, due to the overcorrection of the trim angle that prevented proper ventilation of the forward interceptor at $Fr_B = 3$, the length of the transom interceptor is reduced to $0.25B_{WL}$. Therefore, the results presented for the DIS in planing mode refer to hull performance in wave condition 1, with a transom interceptor height of 2 mm and a length of $0.25B_{WL}$, and a forward interceptor with a length of B_{WL} and height of 2 mm, located 0.8 m from the transom.

Afterwards, the forward interceptor is removed, and the tests are repeated for a hull with a transom interceptor, with a length of $0.25B_{WL}$ and a height of 2 mm at $Fr_B = 3$ in wave condition 1. A comparison of the obtained results for the bare hull, the hull with DIS, and the hull with TIS examines the efficiency of suggested configurations in improving the dynamic performance of HSPC and human safety in planing mode.

4.1. Data representation

Although the generated wave spectra for testing the bare hull are the same as for the hull equipped with an interceptor system, the time history of wave elevation may differ. Therefore, the efficiency of the interceptor system is analyzed through statistical distribution.

A sample of recorded heave, pitch, and vertical acceleration at the CG and bow in wave condition 1 at $Fr_B = 2.2$ is presented in Fig. A1 in appendix A. The analysis of the interceptor system's effect on the dynamic behavior of HSPC is conducted by comparing statistics of significant heave, pitch, and acceleration heights, as well as their 1/3, 1/10, and 1/100 values. The mean values and associated uncertainties for the presented results are provided in Appendix B.

Significant heave motions, which correspond to the 1/3 highest values in the recorded time history, are calculated by identifying the maximum or minimum points between two zero-crossing points. The heave motion height value is calculated by subtracting consecutive maximum and minimum values. Subsequently, the 1/10, and 1/100 of the highest heave motion heights are determined. A similar process is applied for hull acceleration at the CG and bow, as well as for pitch motions.

It is worth noting that since recorded pitch motions are always positive (bow-up) with no zero-crossing point, the pitch data are shifted downward by the mean pitch values to calculate the significant height of pitch motion.

4.2. Dynamic behavior in irregular waves

4.2.1. Bare hull

Fig. 5 indicates the average total resistance of the bare hull in wave conditions 1, 2, and 3 at different Froude numbers. This figure shows that an increase in hull speed leads to a noticeable rise in hull resistance, while the wave conditions have no significant effect. The negligible effects of wave characteristics on hull resistance at each Froude number can be attributed to the similar wave steepness ($S = 0.065$) maintained for the three wave conditions.

Although the effect of wave height on hull resistance is negligible, it can substantially influence hull motions and human safety. Therefore, it is essential to analyze the effects of sea conditions on hull motions and consequently human safety at varying operational speeds.

A statistical analysis is conducted on random wave conditions 1, 2, and 3 to evaluate dynamic hull performance across various waves and speeds. Fig. 6 presents the non-dimensional $H_{1/3}$, $H_{1/10}$, and $H_{1/100}$ significant heave motions in different sea conditions at various speeds. As shown in Fig. 6, in semi-planing and transient modes ($Fr_B = 1.2$ to 2.2), heave motion in wave conditions 1 and 2 decreases with increased hull speed. However, when entering the planing mode ($Fr_B = 3$), heave motion increases. Additionally, the comparison of heave motion in different waves shows higher motions in wave conditions 1, 2, and 3, respectively, due to the higher wave heights.

Fig. 6 also indicates that, for wave condition 1, $H_{1/10}$ at $Fr_B = 1.2$ and $H_{1/100}$ at $Fr_B = 1.2$, 1.7, and 3 exceed the Hs, indicating higher vertical motions compared to the free surface elevation. In contrast, for wave conditions 2 and 3, $H_{1/3}$, $H_{1/10}$, and $H_{1/100}$ are all below Hs across all speeds.

Fig. 7 shows significant pitch motions in wave conditions 1, 2, and 3 at different speeds. As depicted in Fig. 7, the pitch motion decreases with increasing hull speed in semi-planing and transient modes; however, it increases when the speed reaches the planing mode ($Fr_B = 3$), similar to the observation for heave motion. Furthermore, the pitch angle

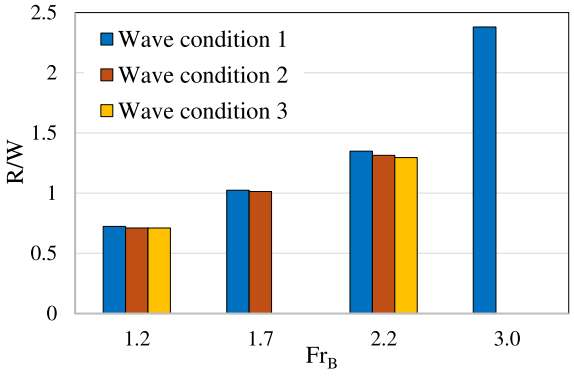

Fig. 5. Nondimensional total resistance in wave conditions 1, 2, and 3 at different Froude numbers.

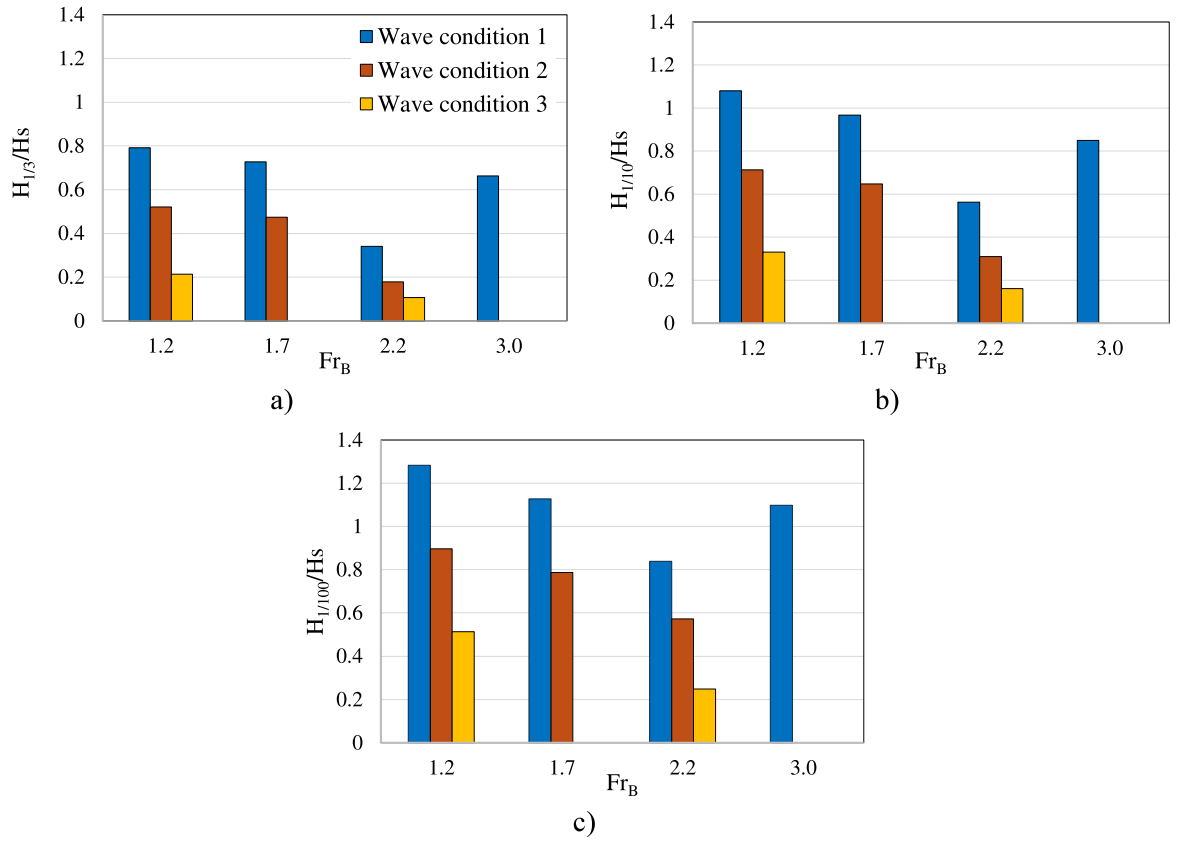

Fig. 6. Significant heave motions for the bare hull in wave conditions 1, 2, and 3 at different Froude numbers: a) $H_{1/3}$, b) $H_{1/10}$, and c) $H_{1/100}$.

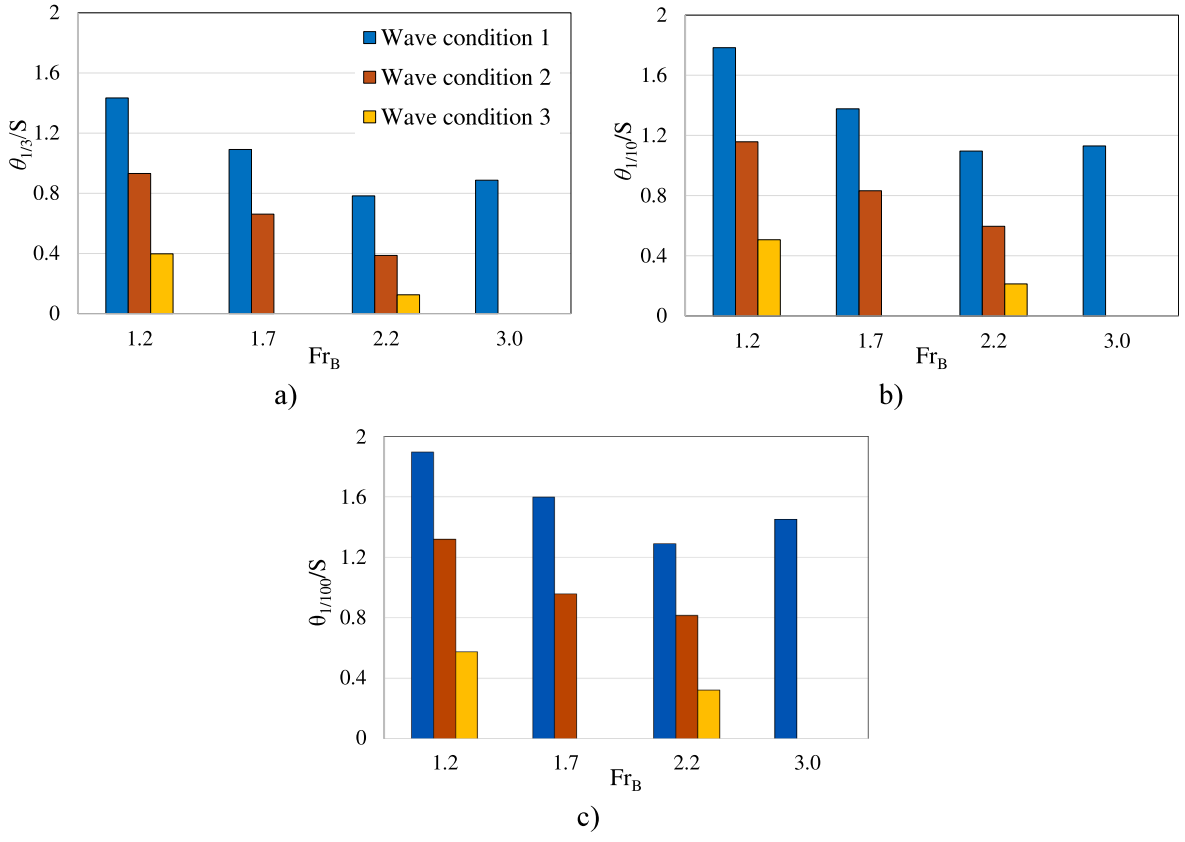

Fig. 7. Significant pitch angles for the bare hull in wave conditions 1, 2, and 3 at different Froude numbers: a) $\theta_{1/3}$, b) $\theta_{1/10}$, and c) $\theta_{1/100}$.

decreases with a reduction in wave height at all examined speeds.

Although undesired hull motion in wave conditions is an important parameter that can affect the HSPC performance, vertical motion acceleration also needs to be considered. Severe vertical impact shocks caused by slam impact could be significant and surpass 20 g (ABCD Group, 2008), with serious effects on crews' safety. Therefore, evaluating and minimizing hull accelerations is crucial to improve HSPC performance and crews' safety. Fig. 8 indicates the significant vertical accelerations on HSPC measured at the bow and CG.

According to Fig. 8, operational speed has a nonlinear effect on vertical accelerations. Comparing vertical acceleration in different wave conditions with a constant steepness indicates that higher accelerations are related to wave conditions 1, 2, and 3, respectively, with higher H_s. Furthermore, a comparison of vertical acceleration and heave motion in Figs. 6 and 8 reveals no similar trend. For instance, in wave condition 1, $a_{1/100}$ at Fr = 1.7 is significantly higher than Fr_B = 1.2, while it has a lower heave motion, as shown in Fig. 6.

According to Fig. 8, the considered hull experiences severe vertical accelerations at Fr_B = 3, exceeding gravitational acceleration. These high accelerations are likely caused by slam impacts, posing significant risks to the hull stability, crew safety, and structural stress. Therefore, minimizing hull motions and accelerations in wave conditions is crucial. The implementation of an interceptor system offers a promising solution to reduce these effects, improving dynamic performance and ensuring higher safety for the crew.

In the subsequent section, the effects of the TIS interceptor $0.5B_{WL}$ on dynamic hull performance in irregular waves at transient mode are analyzed in comparison to the bare hull. To manage the time-consuming nature of irregular wave testing, the evaluation focuses on two wave conditions (wave conditions 1 and 2).

4.2.2. TIS effect on dynamic performance in irregular waves at transient mode

This section analyzes the effects of installing a TIS with a $0.5B_{WL}$ length on the dynamic performance, compared to the bare hull. Fig. 9 shows a comparison between the total resistance of the bare hull and the hull equipped with TIS in wave conditions 1 and 2 during transient mode. According to Fig. 9, the TIS effectively reduces hull resistance. In wave condition 1, hull resistance is reduced by 4.7 % and 4.9 % at Fr_B = 1.7 and 2.2, respectively. A similar trend is observed in wave condition

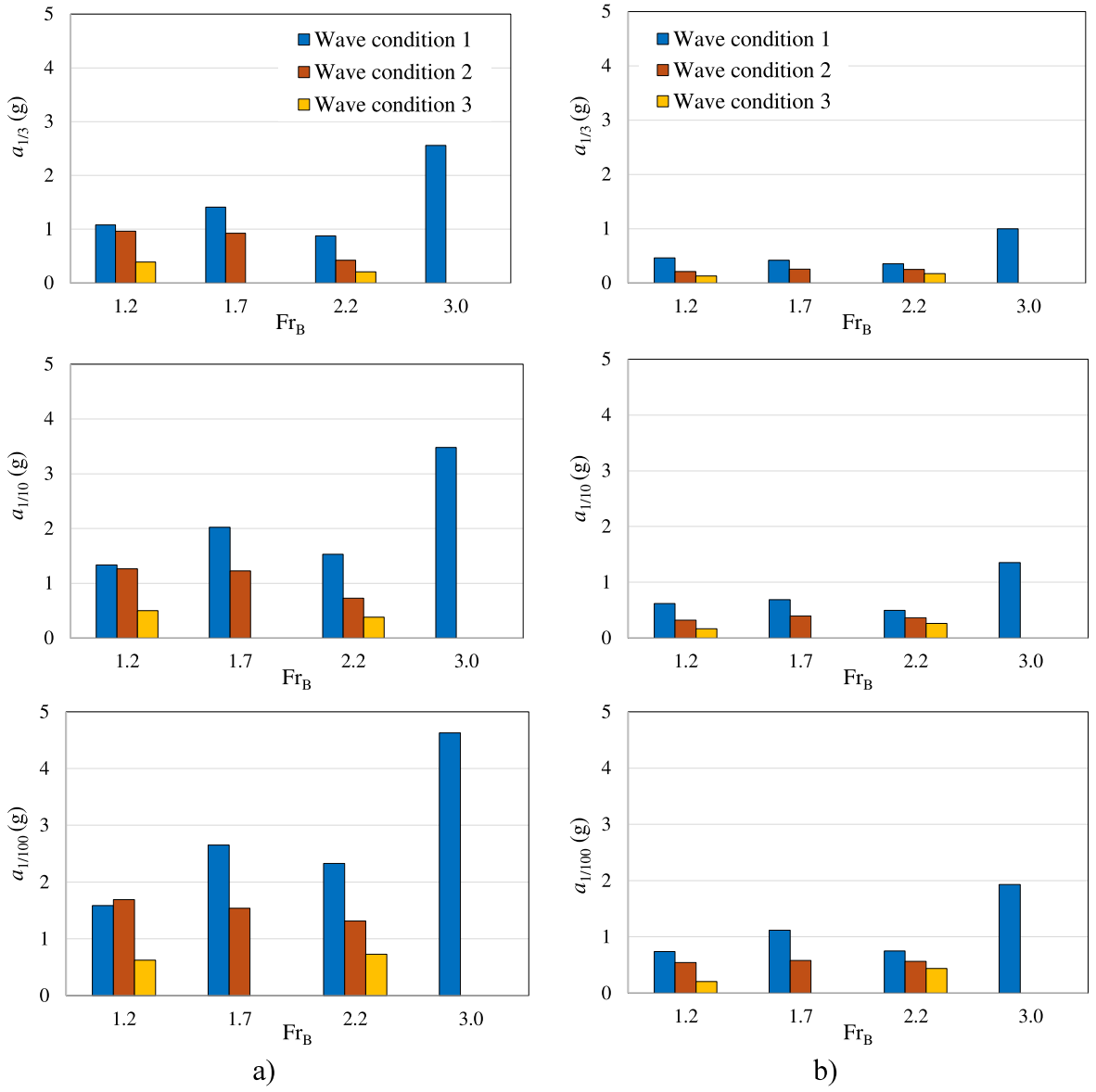

Fig. 8. Non-dimensional significant vertical accelerations for the bare hull in wave conditions 1, 2, and 3 at different Froude numbers: a) $a_{1/3}$, $a_{1/10}$, and $a_{1/100}$ at the bow, and b) $a_{1/3}$, $a_{1/10}$, and $a_{1/100}$ at CG.

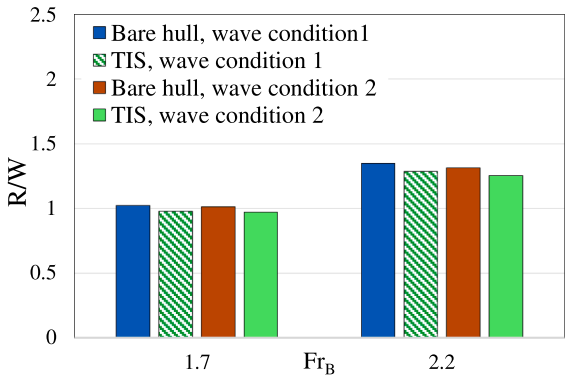

Fig. 9. Hull resistance with and without the TIS ($0.5B_{WL}$) in transient mode for wave conditions 1 and 2.

2, demonstrating the effectiveness of the TIS in transient conditions (detailed results are provided in Appendix C, Table C1).

Fig. 10 provides a statistical analysis of the TIS effect on significant heave motions ($H_{1/3}$, $H_{1/10}$, and $H_{1/100}$) in wave conditions 1 and 2 during transient mode (Fr_B = 1.7 and 2.2). The time history of heave motion at Fr_B = 2.2 under wave conditions 1 and 2, both with and without the TIS are provided in Fig. A2 in Appendix A.

According to Fig. 10, the TIS effectively reduces heave motions in both wave conditions 1 and 2 demonstrating greater efficiency at lower Froude numbers. For instance, $H_{1/3}$ in wave condition 1 at Fr_B = 1.7 is reduced by 59.7 % compared to the bare hull, whereas, at Fr_B = 2.2, the reduction is 13.9 %. Furthermore, reductions at Fr_B = 1.7 in $H_{1/10}$ and $H_{1/100}$ for wave condition 1 are 47.1 % and 27.6 %, respectively. It is evident that the TIS is most effective in reducing moderate heave motions ($H_{1/3}$) compared to extreme values ($H_{1/10}$ and $H_{1/100}$). For detailed information on the percentage of the heave reduction, refer to Table C1 in Appendix C.

As highlighted in previous studies, such as Putra and Suzuki (2024) and John et al., (2011), the implementation of TIS has been shown to effectively reduce the hull trim angle in calm water. This, in turn, influences the pitch motion in wave conditions, as demonstrated by De Luca and Pensa (2014) and Najafi et al. (2015). The time histories of pitch motion at Fr_B = 2.2 under wave conditions 1 and 2 for both the bare hull and hull equipped with TIS are presented in Fig. A3 in Appendix A. As expected, adding TIS causes the hull to rotate around a lower trim angle (reducing the oscillation point for pitch motion), while its effect on reducing pitch amplitude is comparatively limited.

Fig. 11 shows a comparison of $\theta_{1/3}$, $\theta_{1/10}$, and $\theta_{1/100}$ between the bare hull and hull equipped with TIS in transient mode across wave conditions 1 and 2. Further details are provided in Appendix B. Similar to the TIS effect on heave motions, the system is most effective in reducing moderate pitch angles; however, it can amplify higher pitch angles in certain cases. For instance, as shown in Fig. 11, the TIS increases $\theta_{1/100}$ by 7.4 % compared to the bare hull at Fr_B = 1.7 in wave condition 1, while reducing $\theta_{1/3}$ and $\theta_{1/10}$ by 21.4 % and 6.7 %, respectively. A similar trend is observed in wave condition 2, where the TIS achieves the greatest reduction in $\theta_{1/3}$ compared to the $\theta_{1/100}$. Notably, $\theta_{1/100}$ does not increase at this Froude number in wave condition 2, as its value is lower than that in wave condition 1. Detailed reductions for other conditions are available in Table C1 in Appendix C.

In conclusion, the most extreme pitch motions ($\theta_{1/100}$ highest values) provide insight into the most severe events affecting the TIS-equipped hull. Except at Fr_B = 1.7 in wave condition 1, where $\theta_{1/100}$ increases slightly compared to the bare hull, the TIS effectively reduces extreme pitch motions under other conditions. This indicates that the TIS generally improves performance by decreasing the moderate pitch motion occurrences while increasing the severe shocks in rough seas is

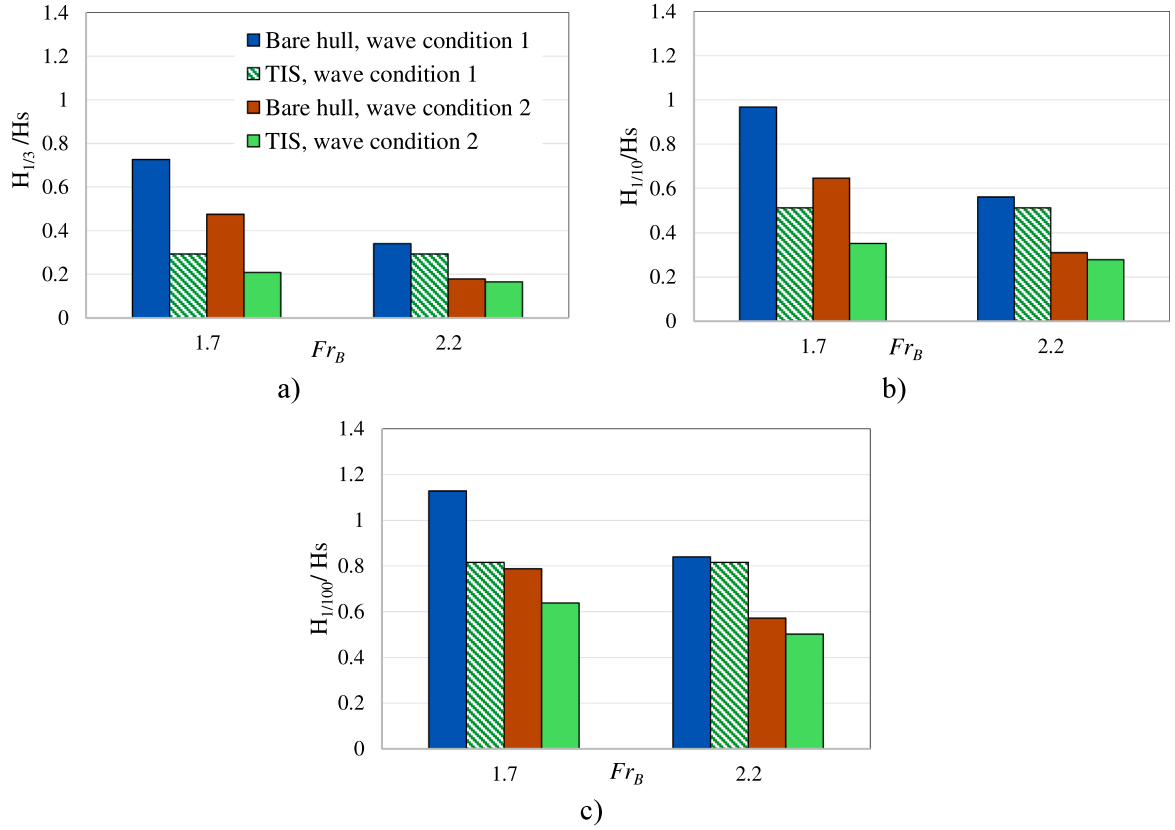

Fig. 10. Non-dimensional significant heave motions for the bare hull and TIS ($0.5B_{WL}$) in transient mode across wave conditions 1 and 2: a) $H_{1/3}$, b) $H_{1/10}$, and c) $H_{1/100}$.

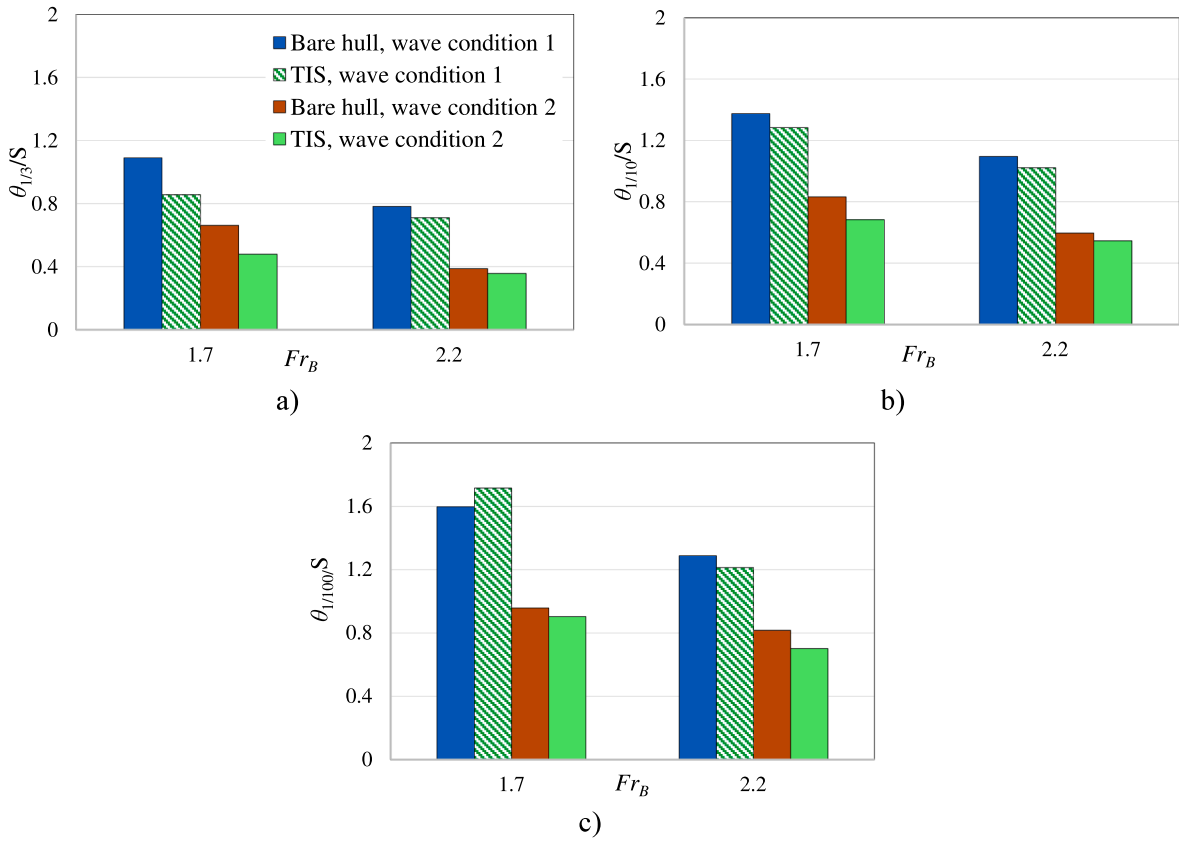

Fig. 11. Non-dimensional significant pitch angle for the bare hull and TIS ($0.5B_{WL}$) in transient mode across wave conditions 1 and 2: a) $\theta_{1/3}$, b) $\theta_{1/10}$, and c) $\theta_{1/100}$.

probable.

Appendix A Fig. A4 presents the time history of vertical acceleration at CG in wave conditions 1 and 2 at $Fr_B = 2.2$ for the bare hull and hull equipped with TIS. Furthermore, a statistical analysis of TIS effect on vertical acceleration at the bow and CG is shown in Fig. 12, with additional details in Appendix B.

As shown in Fig. 12(a), significant bow acceleration in $Fr_B = 1.7$ for the hull equipped with TIS is significantly lower than the bare hull in both sea conditions. Similarly, the TIS reduces bow acceleration in wave 2 at $Fr_B = 2.2$ compared to the bare hull. Nevertheless, in wave 1 at $Fr_B = 2.2$, the $a_{1/100}$ value of bow acceleration, there is an increase from 2.3 g for the bare hull to 2.9 g for the hull with the TIS, posing an increment of potential safety risks to occupants.

Additionally, as Fig. 12(b) shows, the TIS effectively decreases vertical accelerations at CG for wave conditions 1 and 2 at $Fr_B = 1.7$, and for wave 2 at $Fr_B = 2.2$. However, in wave 1 at $Fr_B = 2.2$, TIS leads to an increase in CG acceleration. For instance, the significant CG acceleration $a_{1/10}$ increases by 1.9 % compared to the bare hull. This observation highlights reducing the effectiveness of the TIS at higher speeds in rough water and its potential to amplify motions and accelerations under this condition. Further details can be found in Appendix B and Table C1 in Appendix C.

These findings underscore the need to explore alternative interceptor configurations for improving its performance in planing mode that has higher Froude numbers. To address this, the efficiency of the TIS in improving the dynamic performance of an HSPC in planing mode is compared with DIS performance to identify the most efficient configuration. Based on prior studies (De Luca and Pensa, 2012), it is anticipated that the DIS might demonstrate greater efficiency in reducing hull resistance. In addition, generating an extra lift force by the forward interceptor potentially influences the hull motions and acceleration.

However, experimental tests conducted in calm water revealed that adding a forward interceptor to the current TIS configuration causes an overcorrecting trim angle at $Fr_B = 3$, which prevents proper ventilation of the forward interceptor. Therefore, for investigating TIS and DIS performances in planing mode, the transom interceptor is reduced to $0.25B_{WL}$ to reduce generated bow-down torque by the transom interceptor and avoid overcorrecting trim angle.

4.2.3. TIS and DIS effect on dynamic performance in irregular waves at planing mode

As the results in transient mode demonstrated a decrease in the efficiency of the Transom Interceptor System (TIS) with $0.5B_{WL}$ at higher speeds, two alternative interceptor configurations are tested in planing mode to identify the most effective solution: a TIS with $0.25B_{WL}$, and a Double Interceptor System (DIS), consisting of an interceptor with $0.25B_{WL}$ at the transom and a forward interceptor with the length of 100 % B_{WL} located at 0.8 L_{WL} from the transom. Fig. 13 compares the hull resistance for the bare hull, hull with DIS, and hull with TIS in wave condition 1.

As shown in Fig. 13, the use of DIS results in a 4.6 % increase in hull resistance compared to the bare hull, while the TIS leads to a more significant 23 % increase. The smaller increase in total resistance observed with the DIS is attributed to the forward interceptor's ventilation, which reduces the wetted surface area. Based on these results, neither the DIS nor the TIS configuration reduces hull resistance in planing mode. In the following sections, the effects of these configurations on heave, pitch, and vertical acceleration will be analyzed.

Figs. A5 and A6 in Appendix A, present the effects of TIS and DIS on the time histories of heave and pitch motions in transient mode. Obtained results show that the pitch motion of the hull equipped with TIS oscillates around a lower mean angle compared to the bare hull. However, DIS behaves differently, increasing the trim angle around which the hull rotates.

Fig. 14 presents significant heave and pitch motions for the bare hull, the hull with DIS, and hull with TIS in planing mode. Further details can

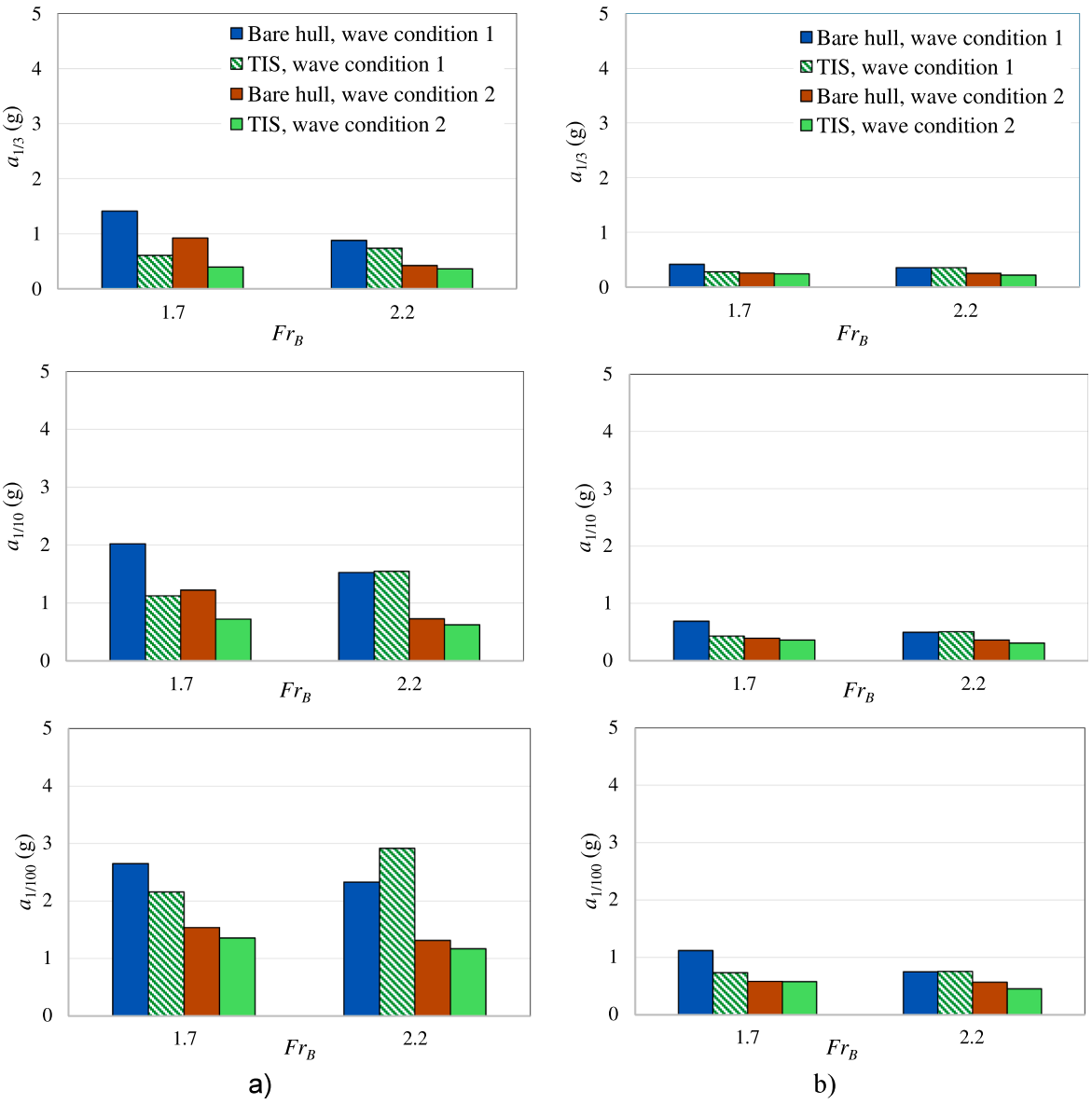

Fig. 12. Non-dimensional significant vertical accelerations for the bare hull and hull equipped with TIS ($0.5B_{WL}$) in transient mode across wave conditions 1 and 2, a) $a_{1/3}$, $a_{1/10}$, and $a_{1/100}$ at the bow, and (b) $a_{1/3}$, $a_{1/10}$, and $a_{1/100}$ at CG.

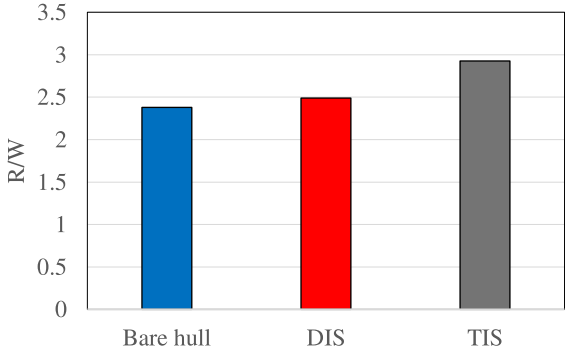

Fig. 13. TIS and DIS effects on hull resistance in wave condition 1 at $Fr_B = 3$.

be found in Appendix B. As shown in Fig. 14, the DIS reduces pitch motions compared to the bare hull, though it leads to an increase in heave motions. In contrast, the TIS effectively reduces both heave and pitch motions when compared to the bare hull. Additionally, a comparison of TIS and DIS performance in reducing pitch motion demonstrates the superiority of TIS. This suggests that the TIS provides a more balanced improvement in dynamic motions. Additional details on the motion reductions can be found in Table C3 in Appendix C. recorded vertical accelerations during the towing tank tests demonstrate that TIS efficiently reduces vertical acceleration at the CG, while DIS has no significant effect. The time history of vertical acceleration for bare hull and hull equipped with TIS and DIS in planing mode is presented Fig. A7 in Appendix A.

Fig. 15 presents significant vertical acceleration at the CG and bow for the bare hull, hull with TIS, and hull with DIS in wave condition 1. Similar to the observed hull motions, the TIS effectively reduces vertical acceleration at both the bow and the CG. In contrast, the DIS amplifies vertical acceleration at both locations. For instance, at the CG, the $a_{1/3}$ acceleration decreases by 45.5 % compared to the bare hull when the TIS is applied, highlighting its significant effect on reducing vertical accelerations. However, when the DIS is used, the $a_{1/3}$ acceleration increases by 12 % compared to the bare hull. This trend is observed at both the CG and bow, with the DIS configuration consistently resulting in higher accelerations. The percentage changes in vertical acceleration for both

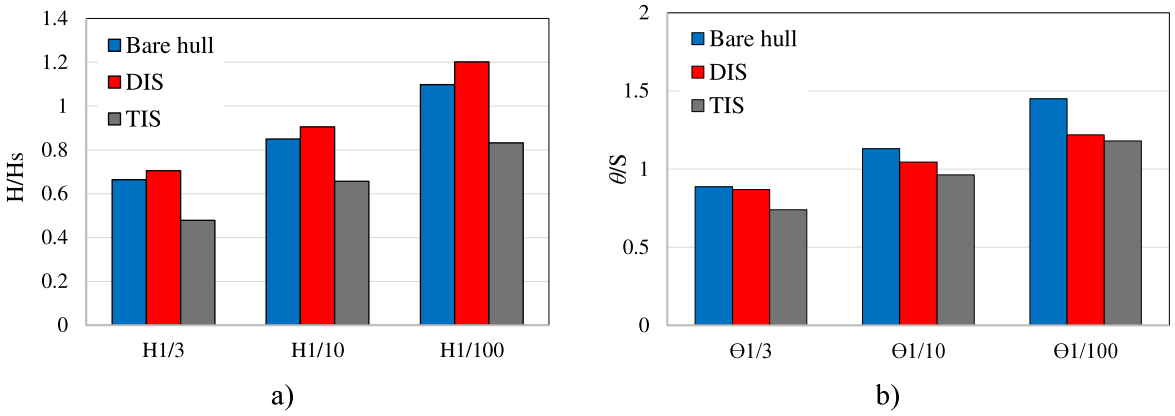

Fig. 14. TIS and DIS performance in reducing a) heave and b) pitch motions in wave condition 1 at Fr_B=3.

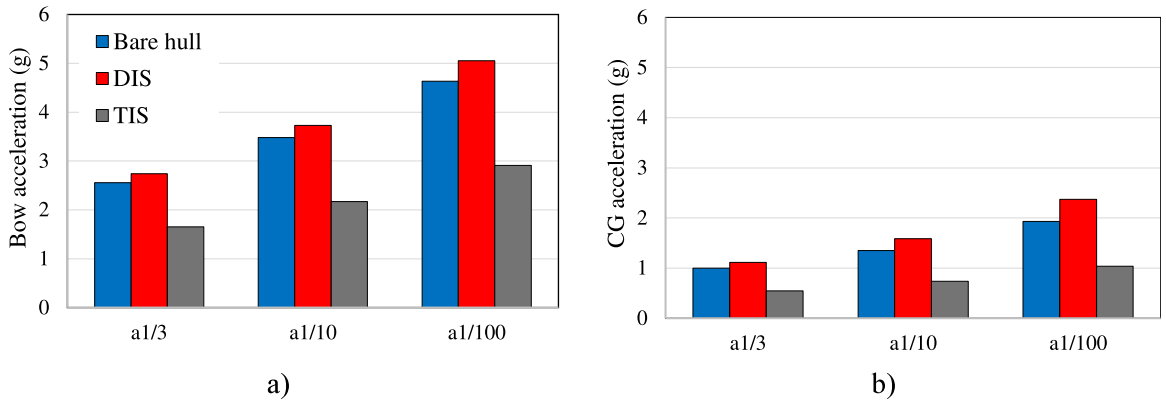

Fig. 15. TIS and DIS performance in reducing hull vertical acceleration at Fr_B = 3 in a) Bow and b) CG.

the DIS and TIS configurations are summarized in Table C3 in Appendix C, providing further insights into the performance of each interceptor system.

The next section evaluates the human safety onboard HSPCs across the considered irregular head wave conditions (wave details are presented in Table 2) at various speeds, regarding ISO 2631-1, (1997); ISO 2631-5, (2004), and EU Directive 2002/44/EC, (2002). These standards provide guidance for assessing the effects of whole-body vibrations (WBV) and shocks on human safety. Therefore, we will apply them to investigate the effects of using different interceptor configurations on improving human safety onboard the HSPC.

4.3. *Human safety onboard the HSPCs*

Ensuring human safety onboard HSPCs is a critical concern, particularly during high-speed operations, as it directly impacts the vessel's operational capabilities. Consequently, investigating the effects of hull accelerations on human health and comfort across various modes and sea conditions is essential.

4.3.1. *Bare hull*

To evaluate the effects of hull accelerations on human comfort, Fig. 16 presents the full-scaled RMS of weighted vertical acceleration at CG and bow for the bare hull across different wave conditions and speeds. According to Fig. 16(a), the RMS decreases as the wave height is

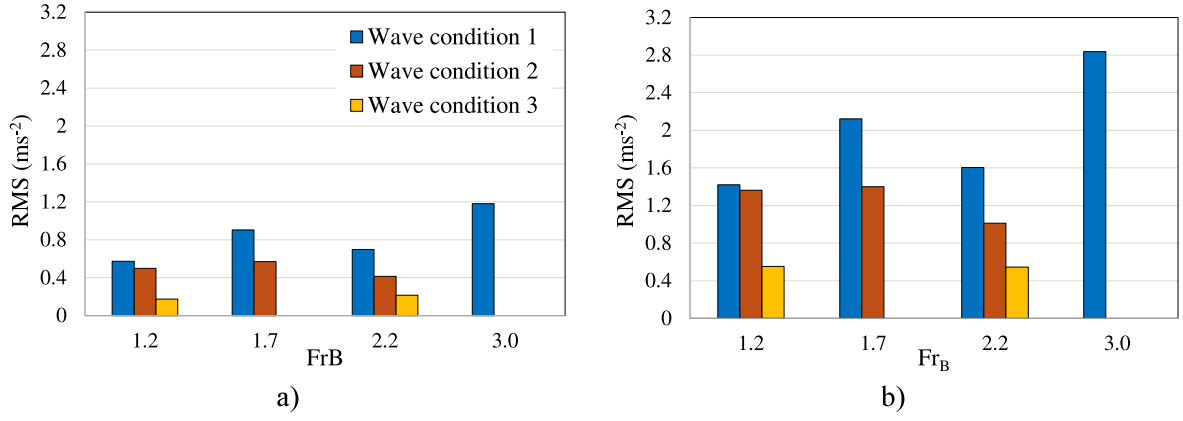

Fig. 16. Weighted RMS acceleration of the bare hull in a) CG and b) bow in wave conditions 1, 2, and 3 at different Froude numbers.

reduced. Consequently, the highest RMS is observed in wave conditions 1, 2, and 3, respectively, at each Froude number.

In wave condition 1, RMS at CG ranges from 0.57 to 1.18 ms^{-2}, while at the bow, it falls between 1.42 and 2.84 ms^{-2}, as evident from Fig. 16. These RMS values at the CG indicate "fairly uncomfortable" to "uncomfortable" conditions for the human, while the values at the bow correspond to "uncomfortable" to "very uncomfortable" conditions, according to [ISO 2631-1, (1997). Furthermore, results obtained in wave conditions 2 and 3 show lower RMS values, demonstrating no serious effects on human comfort at CG. However, RMS at the bow in wave condition 2 could still result in an "uncomfortable" condition, as per ISO 2631-1, (1997). Since HSPCs must be capable of operating in various sea conditions, reducing the vertical acceleration of this hull is essential to improving human comfort, particularly in rough waters.

Although human comfort is an important parameter for HSPCs crews, the risks to human health are even more critical and must also be considered. According to Directive 2002/44/EC, (2002), in the case of high vertical shocks in a vibrated environment, VDV_{8h} can be used to estimate the potential for adverse health effects resulting from WBVs and shocks. Fig. 17 presents full-scaled VDV_{8h} values for the HSPC at CG and bow across different wave conditions and speeds. According to EU Directive 2002/44/EC, (2002), a VDV_{8h} higher than 9.1 $ms^{-1.75}$ indicates an action value for potential health risks, while $VDV_{8h} > 21$ $ms^{-1.75}$ indicates a limit value for adverse health effects.

Fig. 17(a) shows that VDV_{8h} at the CG is significantly lower than the bow. However, under wave condition 1 conditions, it is still higher than the action value at all considered Froude numbers, and it even exceeds the limit value at $Fr_B = 3$ (planing mode). Similarly, VDV_{8h} in wave condition 2 surpasses the action value at $Fr_B = 1.2$ and 1.7, while wave condition 3 exhibits a lower VDV_{8h}, which may indicate a lower probability of health risks due to the lower acceleration intensity.

As shown in Fig. 17(b), VDV_{8h} at the bow exceeds the limit value recommended by EU Directive 2002/44/EC, (2002) in both wave conditions 1 and 2 across all Froude numbers. Additionally, VDV_{8h} in wave condition 3 exceeds the action level at two considered Froude numbers. Although an 8-hour work shift is uncommon for an HSPC, these results demonstrate a significant risk of adverse health effects for crews onboard this HSPC during 8 h of work, especially in planing mode. Therefore, there is a pressing need for safety improvement to reduce the possibility of adverse health risks.

In addition to the possibility of adverse human health risks during HSPCs missions, the long-term negative health effects of vibration exposure can be evaluated using the S_{ed} factor, as recommended by ISO 2631-5, (2004). According to ISO 2631-5, (2004), for a crew aged 20 to 65 years working 220 days a year, $S_{ed} > 0.8$ MPa indicates a high probability of health risks, while $S_{ed} < 0.5$ MPa indicates a low risk. Figs. 18 and 19 present full-scaled $S_{ed,1h}$ and $S_{ed,8h}$ values for daily work onboard this HSPC, considering CG and bow accelerations.

Fig. 18 shows that $S_{ed\text{-}1h}$ and $S_{ed\text{-}8h}$ values are both below the risk threshold in semi-planing and transient mode in wave conditions 1, 2, and 3. However, in planing mode ($Fr_B = 3$), $S_{ed\text{-}1h}$ reaches 0.67 MPa, and $S_{ed\text{-}8h}$ rises to 0.94 MPa, demonstrating a high probability of adverse health effects and underscoring the urgent need to reduce vertical accelerations.

Fig. 19 shows that both $S_{ed\text{-}1h}$ and $S_{ed\text{-}8h}$ values in the bow are below 0.5 MPa at Froude numbers 1.2 and 1.7 across three wave conditions, which is generally considered a low risk for adverse health effects according to ISO 2631-5, (2004). However, at Fr = 2.2, $S_{ed\text{-}1h}$ reaches 1.34 MPa in wave condition 1, indicating high probability of health risks and 0.59 MPa in wave condition 2, indicating probable health risks. Furthermore, at $Fr_B = 3.0$, $S_{ed\text{-}1h}$ increases significantly upon entering the planing regime, reaching 2.45 MPa in wave condition 1, which predicts a high likelihood of long-term negative health effects.

Given that S_{ed} values increase with increasing acceleration exposure time (as seen when comparing $S_{ed\text{-}1h}$ and $S_{ed\text{-}8h}$ in Figs. 18 and 19), reducing exposure duration or implementing acceleration reduction devices becomes essential at higher speeds to reduce human health risks.

The assessment of adverse health effects and discomfort due to hull accelerations highlights the critical need for effective acceleration reduction strategies, particularly in demanding operational scenarios such as high-speed operation in rough sea conditions. For this aim, the TIS has shown promise in reducing accelerations, as observed results in Section 4.2 indicate. To better understand the interceptor's potential for enhancing crew safety, the following section investigates the TIS's impact on safety improvement during transient mode operations, where hull performance is particularly sensitive to wave interactions and speed variations.

4.3.2. *TIS effect on safety improvement in transient mode*

The effects of the TIS on vertical acceleration in transient mode operations have direct implications for human safety onboard HSPCs. To evaluate the TIS's effect on human comfort, a comparison of the full-scaled weighted RMS acceleration of the hull with and without the TIS is presented in Fig. 20 for both the CG and bow.

As shown in Fig. 20, the TIS significantly reduces RMS acceleration at both the CG and bow in transient mode. Specifically, RMS acceleration at the CG decreases by 40.1 % and 36.8 % in wave conditions 1 and 2, respectively, compared to the bare hull at a Froude number of 1.7. Similarly, RMS acceleration at the bow reduces by 43.2 % and 43.9 % relative to the bare hull under the same conditions.

At a higher Froude number of 2.2, the TIS continues to provide a reduction in RMS acceleration, albeit less pronounced. RMS at the CG decreases by 9.6 % and 9.5 %, while RMS at the bow reduces by 11.6 % and 11.3 % in wave conditions 1 and 2, respectively. These results demonstrate that the TIS successfully enhances crew comfort onboard HSPCs during transient mode. However, its effects are notably more

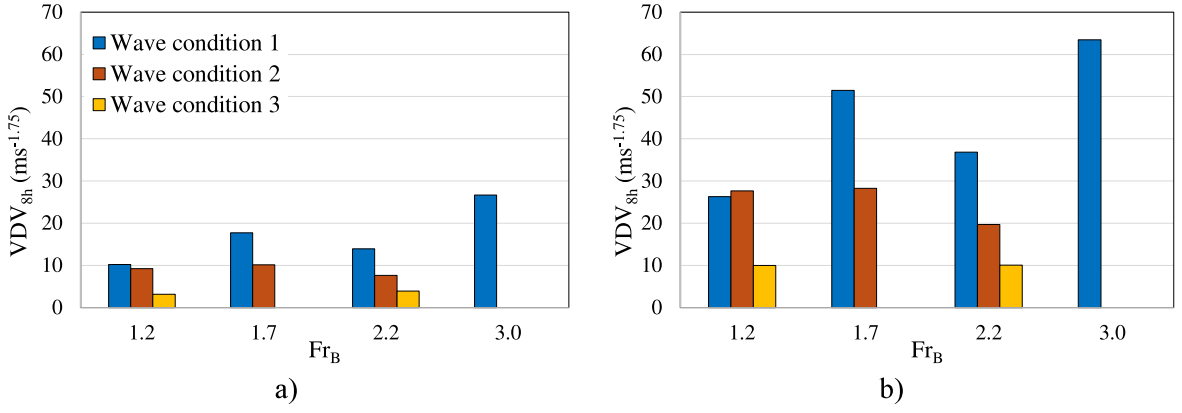

Fig. 17. VDV_{8h} for weighted acceleration in a) CG and b) bow in wave conditions 1, 2, and 3 at different Froude numbers.

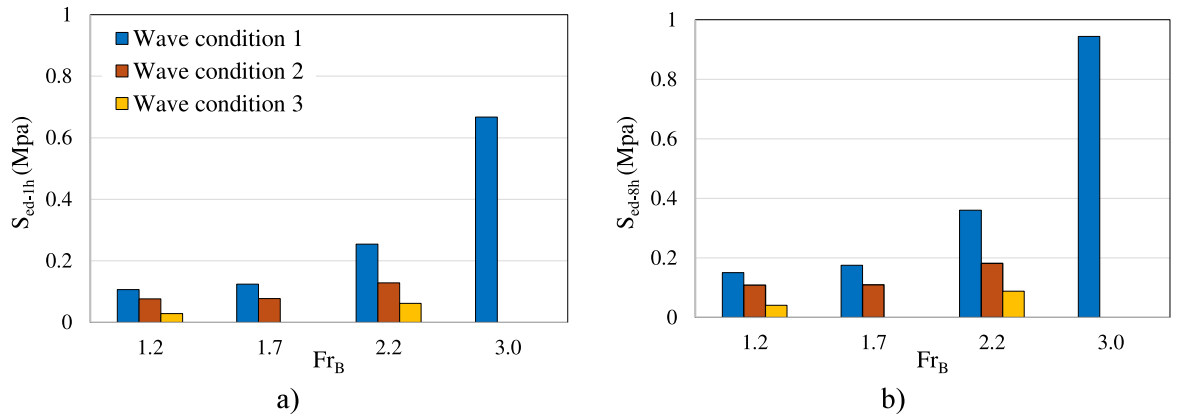

Fig. 18. a) $S_{ed\text{-}1\ h}$, and b) $S_{ed\text{-}8\ h}$ values of weighted accelerations in CG in wave conditions 1, 2, and 3 at different Froude numbers.

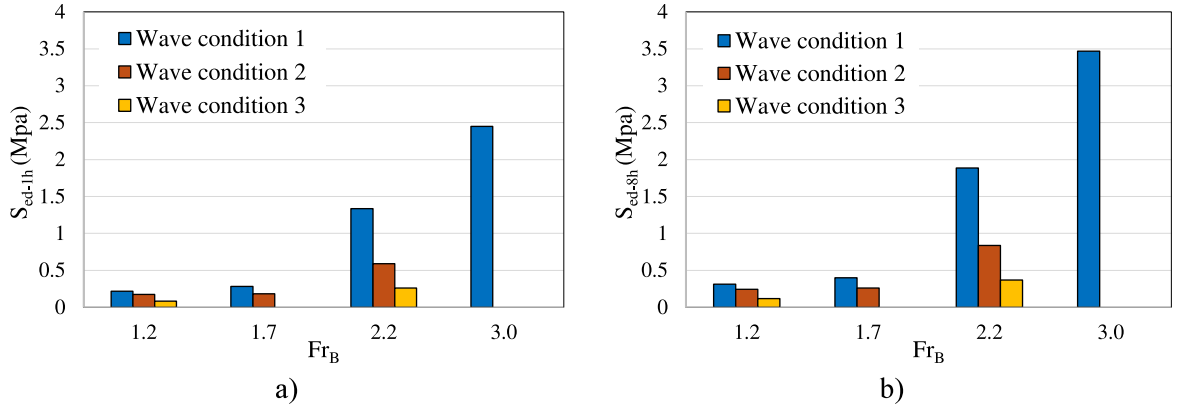

Fig. 19. a) $S_{ed\text{-}1\ h}$, and b) $S_{ed\text{-}8\ h}$ values of weighted accelerations at bow in wave conditions 1, 2, and 3 at different Froude numbers.

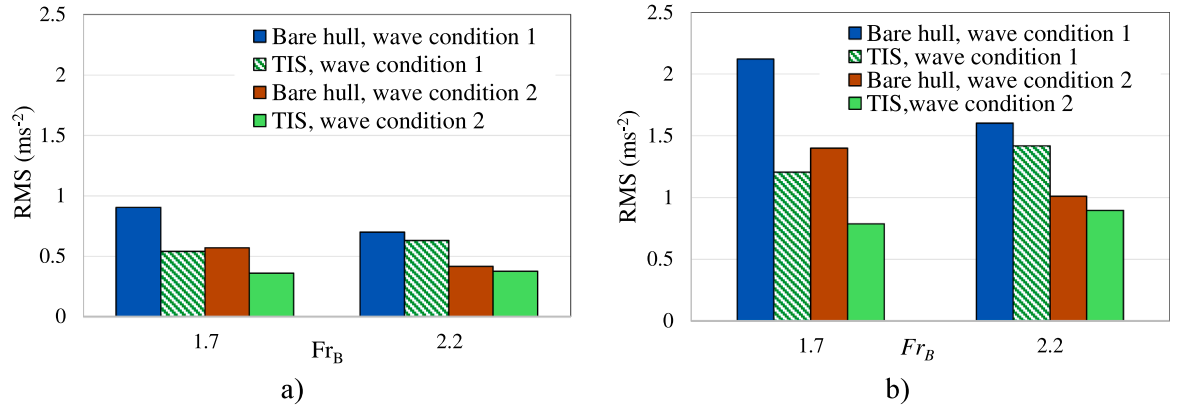

Fig. 20. Weighted RMS acceleration in a) CG and b) bow of the bare hull and hull with a TIS ($0.5B_{WL}$) in transient mode across wave conditions 1 and 2.

substantial at lower speeds, where the influence of the TIS is most effective.

Fig. 21 presents the full-scaled VDV_{8h} value at the CG and bow for the hull with and without the TIS in wave conditions 1 and 2 during the transient mode. The results indicate a significant reduction in VDV_{8h} at both CG and bow when TIS is employed. For instance, at $Fr_B = 1.7$, the VDV_{8h} at the CG and bow decreases by 38.2 % and 45.1 %, respectively, compared to the bare hull under wave condition 1. Similarly, for wave condition 2, the reductions are 36.0 % at the CG and 42.2 % at the bow. These results highlight the TIS's notable capability in improving on-board crews' safety, especially at lower speeds.

Although the TIS effectively reduces VDV_{8h} values at both the CG and bow in wave conditions 1 and 2, its efficiency reduces at higher speeds. For instance, at $Fr_B = 2.2$, the percentage reductions are smaller compared to those observed at $Fr_B = 1.7$, as illustrated in Fig. 21. This trend suggests that the TIS's efficiency in reducing vertical shocks decreases as the vessel transitions into higher speed regimes, likely due to reduced flow control effectiveness at the transom.

Further details, including the precise percentage reductions of VDV_{8h} values, are provided in Appendix C, Table C2. These insights emphasize the importance of optimizing TIS design for varying speed ranges to maximize its safety benefits.

Figs. 22 and 23 show the full-scaled $S_{ed\text{-}1h}$ and $S_{ed\text{-}8h}$ values at the CG and bow for both the bare hull and hull equipped with a TIS in wave

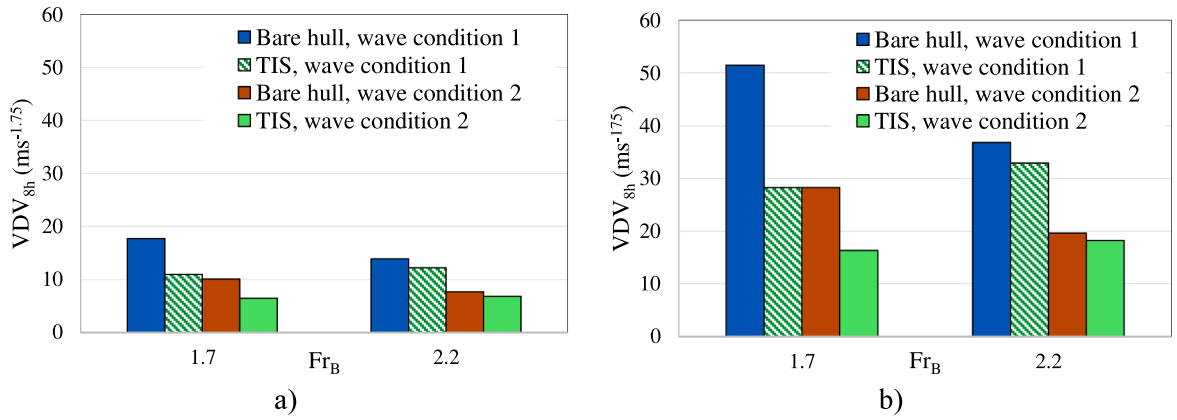

Fig. 21. VDV_{8h} in a) CG and b) bow of the bare hull and hull with a TIS ($0.5B_{WL}$) in transient mode across wave conditions 1 and 2.

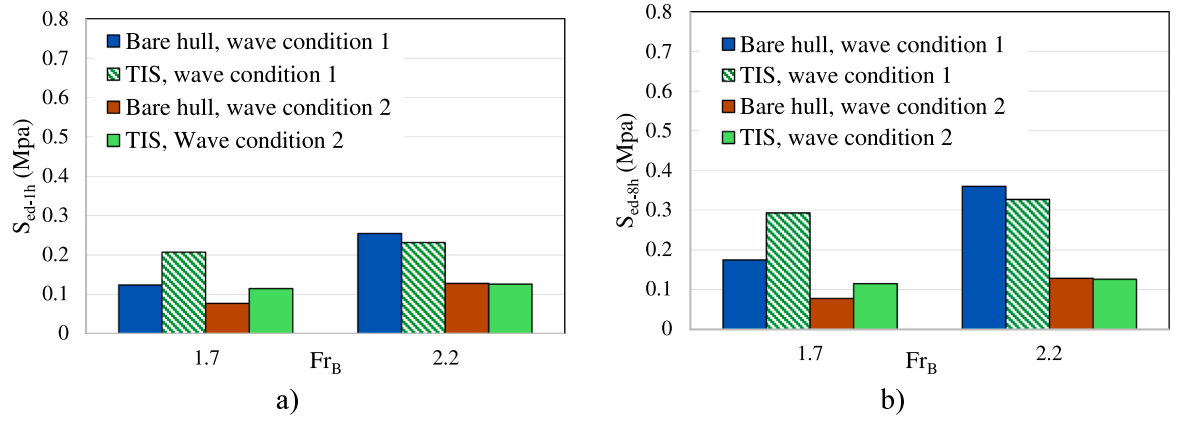

Fig. 22. a). $S_{ed\text{-}1h}$, and b) $S_{ed\text{-}8h}$ in CG for the bare hull and hull with a TIS ($0.5B_{WL}$) in transient mode across wave conditions1 and 2.

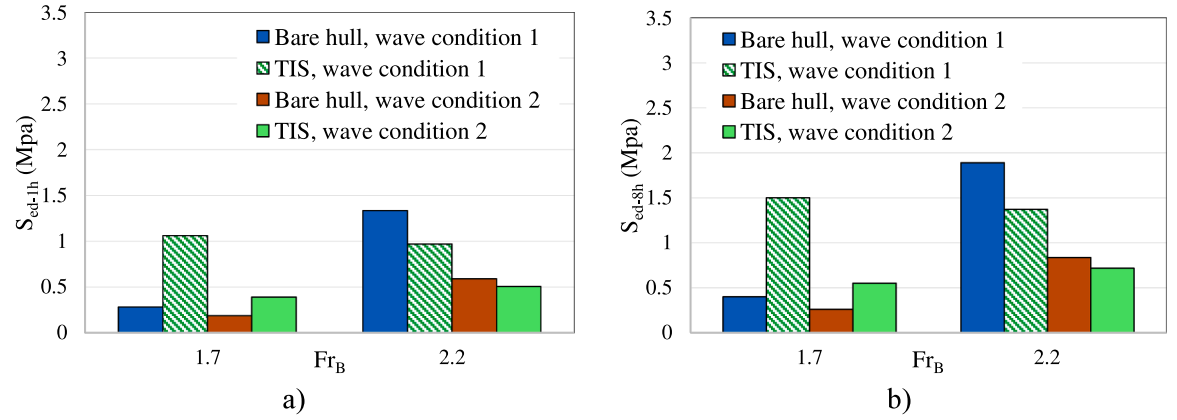

Fig. 23. a). $S_{ed\text{-}1h}$, and b) $S_{ed\text{-}8h}$ in bow for the bare hull and hull with a TIS ($0.5B_{WL}$) in transient mode across wave conditions 1 and 2.

conditions 1 and 2 during the HSPC operation in transient mode. While Figs. 20 and 21 indicated that TIS is more efficient in reducing RMS and VDV_{8h} at lower speeds, it amplifies acceleration effects on the human spine at lower Froude numbers, as evidenced in Figs. 22 and 23.

According to Fig. 22, at $Fr_B = 1.7$, the use of the TIS increases S_{ed} at the CG by 67.2 % and 47.9 % in wave conditions 1 and 2, respectively, compared to the bare hull. Despite this increase, the S_{ed} value for a hull equipped with a TIS at $Fr_B = 1.7$ remains below 0.5 MPa, which ISO 2631-5, (2004) categorizes as having a low probability of long-term health risks. In contrast, at $Fr_B = 2.2$, the S_{ed} at the CG decreases by 9.1 % and 1.6 % in wave conditions 1 and 2, respectively, when the TIS is implemented, highlighting its effectiveness at higher speeds.

Fig. 23 shows the TIS's influence on S_{ed} values at the bow. According to Fig. 23, at $Fr_B = 1.7$, S_{ed} at the bow increases significantly, by 275.7 % and 110.0 % in wave conditions 1 and 2, respectively, compared to the bare hull. This substantial increase causes $S_{ed\text{-}8\ h}$ in wave condition 1 to exceed 0.8 MPa, signifying a high probability of adverse long-term health effects for a human stationed near the bow. Conversely, at $Fr_B = 2.2$, the TIS effectively reduces S_{ed} at the bow by 27.2 % and 14.2 % in wave conditions 1 and 2, respectively.

As a conclusion on the effects of the TIS on human safety at $Fr_B = 1.7$, it effectively reduces WBVs and moderate shocks onboard the HSPC, as

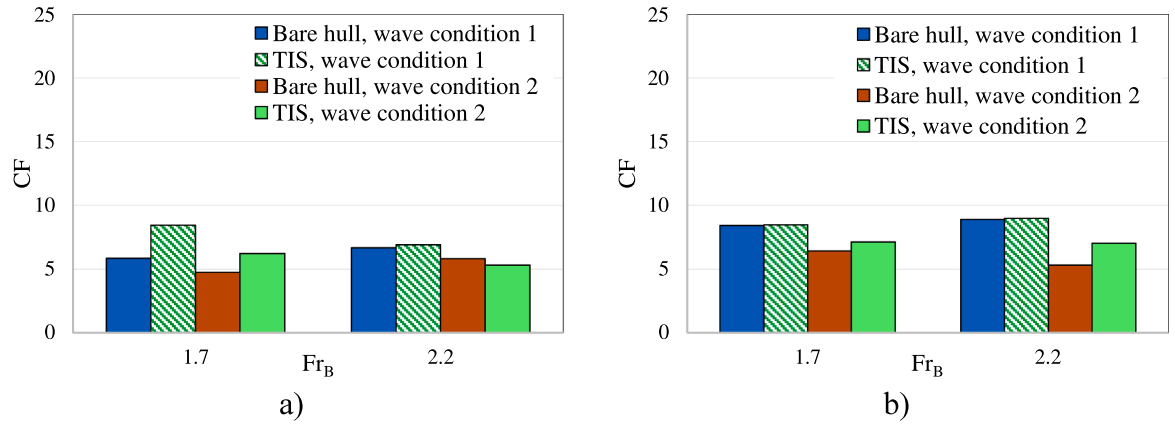

Fig. 24. CF for bare hull and hull with TIS ($0.5B_{WL}$) in a) CG and b) bow in transient mode across wave conditions 1 and 2.

indicated by RMS and VDV_{8h} reduction. However, the TIS may also allow or amplify occasional high acceleration peaks, resulting in an increase in the S_{ed} value. Since S_{ed} is calculated based on the sixth power of weighted acceleration (Eq. (5)), it is highly sensitive to peak acceleration compared to RMS and VDV_{8h}. To further investigate the effect of the TIS on acceleration peak, the full-scaled Crest Factor (CF) for the bare hull and the hull equipped with a TIS is compared in Fig. 24, considering both CG and bow accelerations.

The CF is a nondimensional value defined as the ratio of the maximum weighted acceleration peak to the RMS value. As expected, Fig. 24 shows that TIS amplifies the CF at $Fr_B = 1.7$ in wave conditions 1 and 2, due to an increase in the maximum acceleration peak. This increase in CF correlates with the rise in S_{ed}, even as reductions in RMS and VDV_{8h} indicate decreased WBVs and moderate shocks. In contrast, at $Fr_B = 2.2$, the TIS leads to reductions in CF, S_{ed}, VDV, and RMS across both wave conditions 1 and 2, indicating an overall improvement in human safety at higher speeds.

Up to this point, the analysis is focused on the performance and safety improvement by a TIS with a length of $0.5B_{WL}$ during transient mode operations. This configuration is selected to optimize vertical acceleration reduction at transient mode while ensuring acceptable dynamic performance.

In the next section, the focus shifts to planing mode, where the TIS length are adjusted to $0.25B_{WL}$ to accommodate higher speeds. Additionally, the effects of both the TIS and the DIS are investigated to evaluate their impact on safety improvements and human comfort in this operational regime.

4.3.3. TIS and DIS effect on safety improvement in planing mode

This section investigates the effects of the Transom interceptor system (TIS) with a length of $0.25B_{WL}$ and the DIS on human health and comfort during planing mode operations. As discussed earlier, the TIS length is reduced from $0.5B_{WL}$ to $0.25B_{WL}$ to better accommodate the higher speeds characteristic of planing conditions. The analysis focuses on assessing the effectiveness of these configurations in improving human safety and enhancing crew comfort during high-speed operations.

Considering the effects of the TIS and DIS on vertical acceleration in planing mode, these systems can also affect the WBV and shocks, which directly affect human safety on board HSPCs. Therefore, a comparison of full-scaled RMS and VDV_{8h} values for the bare hull and hulls equipped with TIS and DIS is presented in Fig. 25, focusing on CG and bow accelerations in wave condition 1 at $Fr_B = 3$.

As shown in Fig. 25, the DIS results in a 6.4 % and 8.7 % increase in RMS and VDV_{8h} of weighed CG accelerations, respectively, compared to the bare hull. Similarly, there is a 0.3 % and 4.7 % increase in RMS and VDV_{8h} for weighted bow acceleration. Although these increases in RMS and VDV are not substantial, it can be concluded that the DIS is not efficient in improving human safety onboard HSPCs in planing mode. In fact, it may even increase the probability of adverse health effects and discomfort in planing mode.

Fig. 25 also indicates that RMS and VDV_{8h} for the hull equipped with TIS are significantly lower than the bare hull. The percentage reductions in RMS and VDV for both CG and bow accelerations are presented in Table C3 in Appendix C. These results suggest that the use of TIS can improve safety by reducing the risks of human comfort and adverse health effects in planing mode. Tables B1, B2, B3.

The effects of using TIS and DIS on long-term negative health effects in planing mode are investigated by comparing the full-scaled S_{ed} values for the bare hull, the hull equipped with TIS, and the hull equipped with DIS, as shown in Fig. 26. According to Fig. 26, the use of DIS increases S_{ed} by 18.8 % in the CG compared to the bare hull, while its effect on the S_{ed} of the bow is negligible. Moreover, TIS successfully reduces S_{ed} at both CG and bow by 60.6 % and 51.1 %, respectively, highlighting TIS's effectiveness in improving human safety onboard HSPCs.

Fig. 27 shows a comparison of the effect of TIS and DIS on the full-scaled CF of weighted CG and bow accelerations in wave condition 1 at $Fr_B = 3$. As shown in Fig. 27, the use of DIS results in a 12.0 % and 6.6 % increase in CF for the CG and bow, respectively, compared to the bare hull. In contrast, TIS increases the CF in the bow by 3.0 %, while it efficiently reduces CF in the CG by 37.1 %.

5. Discussion

This study investigated the effects of Transom Interceptor Systems (TIS) and Double Interceptor Systems (DIS) on the dynamic performance and crew's safety onboard a High-Speed Planing Craft in rough water under varying operational regimes. A bare hull was used as a benchmark to highlight the improvements achieved through these systems. The findings provided a comprehensive evaluation of wave-induced motions, hull accelerations, and human safety risks, focusing on weighted root-mean-square (RMS), vibration dose value (VDV), and spine dose value (S_{ed}) indices as defined by ISO 2631-1, (1997); ISO 2631-5, (2004), and EU Directive 2002/44/EC, (2002) standards.

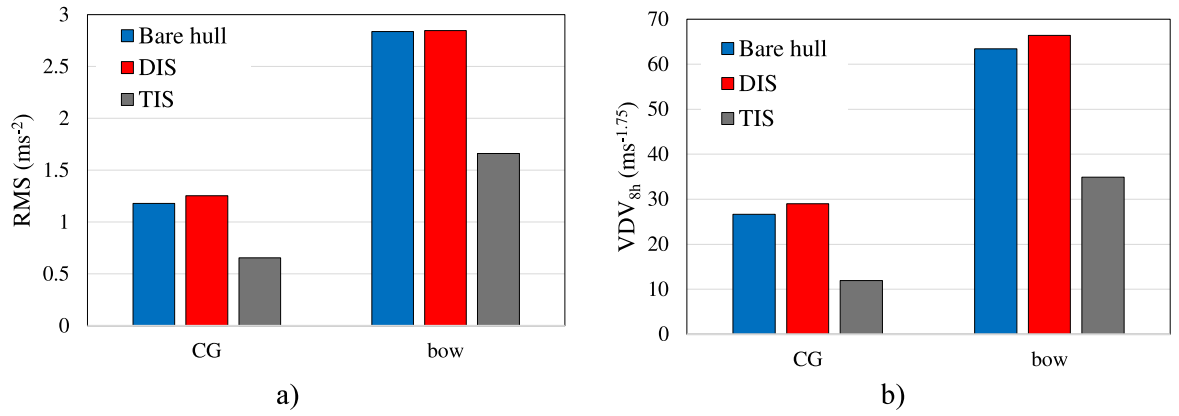

Fig. 25. TIS and DIS effects in a) RMS and b) VDV_{8h} of weighted CG and bow acceleration in wave condition 1 at Fr_B= 3.

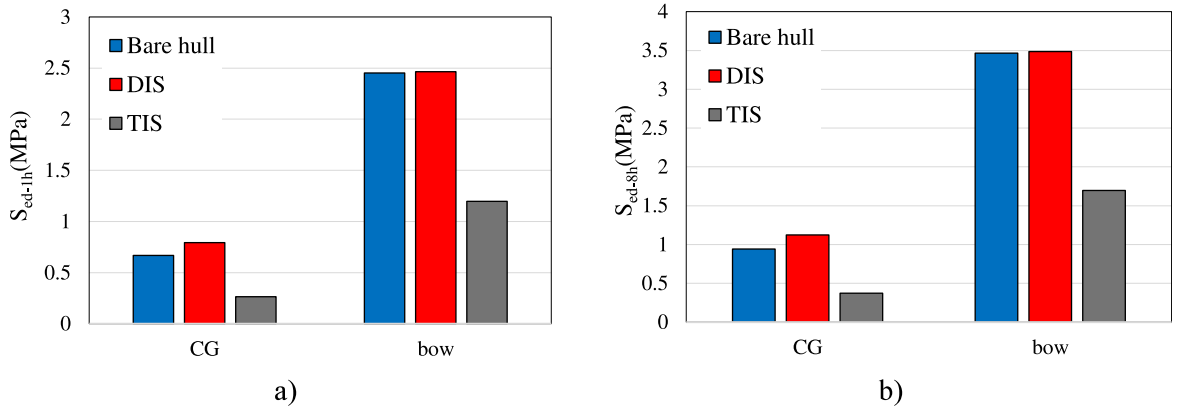

Fig. 26. TIS and DIS effects in a) $S_{ed\text{-}1h}$ and b) $S_{ed\text{-}8h}$ in wave condition 1 and Fr_B=3.

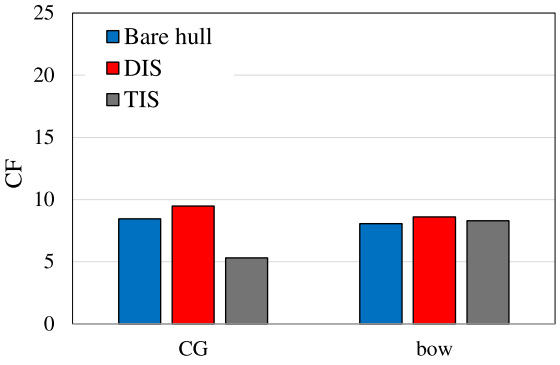

Fig. 27. TIS and DIS effects in crest factor in wave condition 1 at Fr_B = 3.

The results show that TIS, particularly when optimized for specific speed regimes, significantly improves dynamic performance and crew safety. In transient mode, a TIS length of $0.5B_{WL}$ was shown to be effective in reducing hull resistance, heave, and pitch motions, as well as moderate accelerations. Consequently, reducing vertical accelerations resulted in a decrease in RMS and VDV_{8h} values, reducing potential human health and comfort risks. However, it occasionally increased S_{ed} values due to sensitivity to peak accelerations.

In planing mode, reducing the TIS length to $0.25B_{WL}$ provided substantial advantages by reducing hull heave and pitch motions, vertical acceleration, RMS, VDV8h, and S_{ed} values across CG and bow accelerations. This observation highlights the TIS efficacy in improving the dynamic performance of an HSPC and enhancing human safety at higher speeds. However, it should be noted that implementing TIS in planing mode leads to an increase in total resistance.

Conversely, the DIS showed limited efficiency in improving dynamic performance and human safety while offering some dynamic benefits in reducing pitch motion. In planing mode, DIS slightly increased hull resistance, heave motion, vertical acceleration, RMS, and VDV_{8h} values at both CG and bow, along with S_{ed} values in the CG region. These findings suggest that employing DIS to improve dynamic and human safety in planing mode requires further refinements.

Current results align with the results of Park et al., (2019) which highlighted the effects of TIS on HSPC dynamics under irregular wave conditions. Additionally, the performance of DIS has been previously examined in regular wave by De Luca and Pensa (2011), who indicated a potential increase in hull motions. We specifically focused on the effect of TIS and DIS on human safety by analyzing their influence on hull motions and accelerations in irregular wave conditions.

This study is limited to three irregular head waves and four Froude numbers, which may not fully represent the range of operational environments encountered by HSPCs. Furthermore, the analysis considers only three degrees of freedom, neglecting other motions that could affect hull responses and human safety. Addressing these limitations in future research will enhance the generalizability of the findings.

6. Conclusion

This study analyzed the effects of using TIS and DIS on the dynamics of HSPC and their role in improving human safety by reducing accelerations. Towing tank tests are conducted at the Università degli Studi di Napoli "Federico II" providing high-fidelity data that captured the nuances of hull performance in semi-planing, transient, and planing modes. The experiments utilized advanced equipment, including triaxial accelerometers for measuring hull accelerations and motion capture systems for tracking hull responses in wave conditions. These facilities ensure accurate and reliable data to support the analysis.

The findings indicate that in both transient and planing modes, the TIS can efficiently reduce hull motions and accelerations and consequently enhance human safety. However, the measured data for DIS performance in planing mode showed higher motions and accelerations compared to the bare hull.

These results provide a new insight into the efficiency of interceptor systems in enhancing human safety, which can consider in designing and implementation of effective interceptor system. However, the scope of this study is limited to HSPC dynamics under the three degrees of freedom (surge, heave, and pitch) in three irregular head wave conditions at different speeds, along with specific interceptor system configurations. Future research could investigate the effects of interceptor on lateral motions and accelerations, considering waves from other directions and hull with unrestricted sideways motions. Furthermore, a more detailed analysis of fluid flow around the hull could be achieved by simulating HSPC with advanced computational methods.

CRediT authorship contribution statement

Fatemeh Roshan: Writing – original draft, Resources, Formal analysis, Data curation, Methodology, Conceptualization, Visualization, Investigation. **Rasul Niazmand Bilandi:** Investigation, Writing – review & editing, Formal analysis, Validation, Conceptualization, Resources, Data curation. **Fabio De Luca:** Writing – review & editing, Formal analysis, Resources, Data curation. **Simone Mancini:** Supervision, Formal analysis, Writing – review & editing, Data curation. **Pentti Kujala:** Writing – review & editing, Supervision. **Abbas Dashtimanesh:** Writing – review & editing, Supervision, Formal analysis.

Declaration of competing interest

The authors declare that they have no known competing financial interests or personal relationships that could have appeared to influence the work reported in this paper.

Acknowledgments

This study was supported by the Research Project PRIN_2022PNRR_P2022Y3PBY_001 "MADELEINE", CUP J53D23001980006, and projects funded under the National Recovery and Resilience Plan (NRRP), Mission 4 Component C2 Investment 1.1 by the European Union—NextGenerationEU.

Appendix A

Para

Appendix B

To minimize aliasing errors and identify any identify any unintended sources of error from the acquisition system, a high sampling rate is applied using the oversampling technique. As a result, a standard rate of 500 Hz—ten times the network frequency—is selected. In the benchmark study of the NSS series, De Luca and Pensa (2017) previously applied ITTC 7.5–02–02–02 to evaluate the total measurement uncertainty during towing tank tests of the NSS hull series. Their reported total uncertainties in resistance measurement are ±0.01 N, ±0.05° on trim, ±0.001 m/s on speed, and±0.01 kg on weights. Additionally, interceptor height is measured with an uncertainty of 0.02 mm. The uncertainties related to the weights for model C5 can be found in De Luca and Pensa (2017).

The mean value of significant hull motions and accelerations and the uncertainty of the mean value are calculated in accordance with ITTC 7.5–02–01–01, using following equations:

$$\overline{q} = \frac{1}{N}\sum_{t=0}^{T} q(t) \tag{B1}$$

N is the number of data points in the top *1/n* portion (e.g., 1/3, 1/10, or 1/100), T is the measurement time, and *q(t)* represents a time series of a uniformly sampled quantity (e.g., heave, pitch, or acceleration) that top 1/n subset, and $\overline{q}$ is the mean value of the quantity. Furthermore, the standard deviation of q is calculated by:

$$S = \sqrt{\frac{1}{N-1}\sum_{t=0}^{T}(q(t)-\overline{q})^2} \tag{B2}$$

Then the standard uncertainty is estimated as:

$$u(\overline{q}) = \frac{S}{\sqrt{N}} \tag{B3}$$

To consider a 95 % confidence interval, the following equation is used:

$$\overline{q} \pm 1.96.u(\overline{q}) \tag{B4}$$

Table B1
Obtained results and uncertainty for the bare hull.

Wave. No	Fr_B	Heave/Hs			*Pitch/S*			CG acceleration (g)			Bow acceleration (g)		
		$H_{1/3}$	$H_{1/10}$	$H_{1/100}$	$\theta_{1/3}$	$\theta_{1/10}$	$\theta_{1/100}$	$A_{1/3}$	$A_{1/10}$	$A_{1/00}$	$A_{1/3}$	$A_{1/10}$	$A_{1/00}$
1	1.2	0.79 ±0.04	1.08 ±0.04	1.28 ±0.03	1.43 ±0.06	1.78 ±0.03	1.90 ±0.01	0.47±0.02	0.62 ±0.03	0.74±0.04	1.08 ±0.04	1.34 ±0.05	1.59 ±0.03
1	1.7	0.73 ±0.04	0.97 ±0.03	1.13 ±0.01	1.09 ±0.05	1.38 ±0.05	1.60 ±0.01	0.42±0.03	0.69 ±0.04	1.12±0.05	1.41 ±0.09	2.02 ±0.13	2.65 ±0.06
1	2.2	0.34 ±0.02	0.56 ±0.02	0.84 ±0.02	0.78 ±0.03	1.10 ±0.02	1.29 ±0.05	0.36 ±0.004	0.49 ±0.01	0.75±0.03	0.88 ±0.04	1.53 ±0.06	2.33 ±0.10
1	3.0	0.66 ±0.03	0.85 ±0.05	1.10 ±0.01	0.89 ±0.04	1.13 ±0.05	1.45 ±0.10	1.00±0.04	1.35 ±0.07	1.93±0.10	2.56 ±0.12	3.48 ±0.15	4.63 ±0.18
2	1.2	0.52 ±0.02	0.71 ±0.03	0.90 ±0.02	0.93 ±0.03	1.16 ±0.04	1.32 ±0.01	0.21±0.01	0.32 ±0.01	0.54±0.04	0.97 ±0.04	1.26 ±0.06	1.69 ±0.06
2	1.7	0.44 ±0.02	0.60 ±0.02	0.73 ±0.01	0.66 ±0.02	0.83 ±0.02	0.96 ±0.02	0.26±0.01	0.39 ±0.01	0.58±0.03	0.92 ±0.04	1.22 ±0.05	1.54 ±0.10
2	2.2	0.16 ±0.01	0.29 ±0.01	0.53 ±0.02	0.39 ±0.02	0.60 ±0.03	0.82 ±0.03	0.25 ±0.003	0.36 ±0.01	0.57±0.02	0.42 ±0.02	0.73 ±0.04	1.32 ±0.12
3	1.2	0.21 ±0.01	0.33 ±0.01	0.51 ±0.02	0.40 ±0.01	0.51 ±0.01	0.57 ±0.01	0.13±0.00	0.16 ±0.01	0.21 ±0.004	0.39 ±0.01	0.50 ±0.02	0.63 ±0.03
3	2.2	0.11 ±0.00	0.16 ±0.00	0.25 ±0.01	0.13 ±0.01	0.21 ±0.01	0.32 ±0.01	0.17±0.00	0.26 ±0.00	0.44±0.02	0.21 ±0.01	0.38 ±0.02	0.73 ±0.04

Table B2
Obtained results and uncertainty for the hull with TIS.

Wave. No	Fr_B	Heave/Hs			*Pitch/S*			CG acceleration (g)			Bow acceleration (g)		
		$H_{1/3}$	$H_{1/10}$	$H_{1/100}$	$\theta_{1/3}$	$\theta_{1/10}$	$\theta_{1/100}$	$A_{1/3}$	$A_{1/10}$	$A_{1/00}$	$A_{1/3}$	$A_{1/10}$	$A_{1/00}$
1.0	1.7	0.33 ±0.02	0.58 ±0.03	0.97 ±0.06	0.86 ±0.05	1.28 ±0.07	1.72 ±0.07	0.26 ±0.01	0.41 ±0.01	0.71 ±0.04	0.60 ±0.04	1.10 ±0.09	2.25 ±0.19
1.0	2.2	0.29 ±0.02	0.51 ±0.03	0.82 ±0.02	0.71 ±0.03	1.02 ±0.03	1.21 ±0.03	0.36 ±0.00	0.50 ±0.01	0.75 ±0.02	0.74 ±0.06	1.54 ±0.10	2.95 ±0.10
1.0	3.0	0.48 ±0.03	0.66 ±0.04	0.83 ±0.01	0.74 ±0.03	0.96 ±0.05	1.18 ±0.04	0.54 ±0.02	0.74 ±0.04	1.04 ±0.08	1.65 ±0.07	2.17 ±0.10	2.91 ±0.57
2.0	1.7	0.19 ±0.01	0.32 ±0.01	0.59 ±0.04	0.48 ±0.02	0.68 ±0.02	0.90 ±0.01	0.24 ±0.00	0.36 ±0.01	0.58 ±0.02	0.39 ±0.02	0.72 ±0.04	1.36 ±0.05
2.0	2.2	0.15 ±0.01	0.26 ±0.01	0.46 ±0.02	0.36 ±0.02	0.55 ±0.02	0.72 ±0.02	0.22 ±0.00	0.31 ±0.00	0.45 ±0.01	0.36 ±0.01	0.63 ±0.03	1.17 ±0.08

Table B3
Obtained results and uncertainty for the hull with DIS.

Wave. No	Fr_B	Heave/Hs			*Pitch/S*			CG acceleration (g)			Bow acceleration (g)		
		$H_{1/3}$	$H_{1/10}$	$H_{1/100}$	$\theta_{1/3}$	$\theta_{1/10}$	$\theta_{1/100}$	$A_{1/3}$	$A_{1/10}$	$A_{1/00}$	$A_{1/3}$	$A_{1/10}$	$A_{1/00}$
1.0	3.0	0.70 ±0.03	0.91 ±0.05	1.20 ±0.00	0.87 ±0.03	1.05 ±0.04	1.25 ±0.04	1.12 ±0.06	1.59 ±0.09	2.37 ±0.23	2.74 ±0.14	3.73 ±0.18	5.06 ±0.22

Appendix C

Table C1
A summary of TIS $0.5B_{WL}$ effect in dynamic performance of an HSPC in waves 1 and 2 at transient mode ($Fr_B = 1.7$ and 2.2).

Wave number	Fr_B	Resistance reduction	Heave reduction			Pitch reduction			Acceleration reduction in CG			Acceleration reduction in bow		
			$H_{1/3}$	$H_{1/10}$	$H_{1/100}$	$\theta_{1/3}$	$\theta_{1/10}$	$\theta_{1/100}$	$A_{1/3}$	$A_{1/10}$	$A_{1/100}$	$A_{1/3}$	$A_{1/10}$	$A_{1/100}$
1	1.7	4.7 %	21.4 %	6.7 %	7.4 %	21.4 %	6.7 %	−7.4 %	33.0 %	38.0 %	34.2 %	56.9 %	44.5 %	18.8 %
1	2.2	4.9 %	9.1 %	6.7 %	5.8 %	9.1 %	6.7 %	5.8 %	−0.9 %	−1.9 %	−0.3 %	16.3 %	−1.4 %	−25.3 %
2	1.7	4.2 %	56.4 %	45.6 %	19.0 %	27.7 %	18.0 %	5.6 %	6.1 %	9.1 %	0.7 %	57.4 %	40.9 %	11.8 %
2	2.2	4.7 %	7.2 %	10.3 %	12.2 %	7.6 %	8.3 %	14.1 %	12.4 %	14.5 %	19.7 %	15.2 %	13.7 %	11.1 %

*Negative value means increasing the parameter.

Table C2
A summary of TIS $0.5B_{WL}$ effect in human safety onboard a HSPC in waves 1 and 2 at transient mode ($Fr_B = 1.7$ and 2.2).

Wave number	Fr_B	CF reduction		RMS reduction		VDV reduction		S_{ed} reduction	
		CG	bow	CG	bow	CG	bow	CG	bow
1	1.7	−44.1 %	−0.5 %	40.1 %	43.2 %	38.2	45.1 %	−67.2 %	−275.7 %
1	2.2	−3.5 %	0.8 %	9.6 %	11.6 %	12.1	10.6 %	9.1 %	27.3 %
2	1.7	−31.1 %	−11.1 %	36.8 %	43.9 %	36.0	42.2 %	−47.9 %	−110.0 %
2	2.2	8.32 %	−32.6 %	9.5 %	11.3 %	11.4	7.3 %	1.6 %	14.2 %

*Negative value means increasing the parameter.

Table C3
A summary of TIS $0.25B_{WL}$ and DIS effects on dynamic performance and human safety onboard an HSPC in wave 1 at planing mode ($Fr_B = 3$).

Parameters		TIS	DIS
Resistance	–	23.0 %	−4.6 %
Heave reduction	$H_{1/3}$	27.9 %	−6.2 %
	$H_{1/10}$	22.6 %	−6.6 %
	$H_{1/100}$	24.2 %	−9.5 %
Pitch reduction	$\theta_{1/3}$	16.7 %	2.0 %
	$\theta_{1/10}$	14.9 %	7.6 %
	$\theta_{1/100}$	18.6 %	15.9 %
Acceleration reduction in CG	$A_{1/3}$	45.5 %	−12.0 %
	$A_{1/10}$	45.4 %	−17.2 %
	$A_{1/100}$	46.3 %	−22.6 %
Acceleration reduction in Bow	$A_{1/3}$	35.3 %	−7.2 %
	$A_{1/10}$	37.7 %	−7.1 %
	$A_{1/100}$	37.1 %	−9.2 %
CF reduction	CG	37.1 %	−12.0 %
	Bow	−3.0 %	−6.6 %
RMS reduction	CG	44.4 %	6.4 %
	Bow	41.5 %	0.3 %
VDV reduction	CG	55.3 %	−8.7 %
	Bow	44.9 %	−4.7 %
S_{ed} reduction	CG	60.5 %	−18.8 %
	Bow	51.1 %	−0.6 %

*Negative value means increasing the parameter.

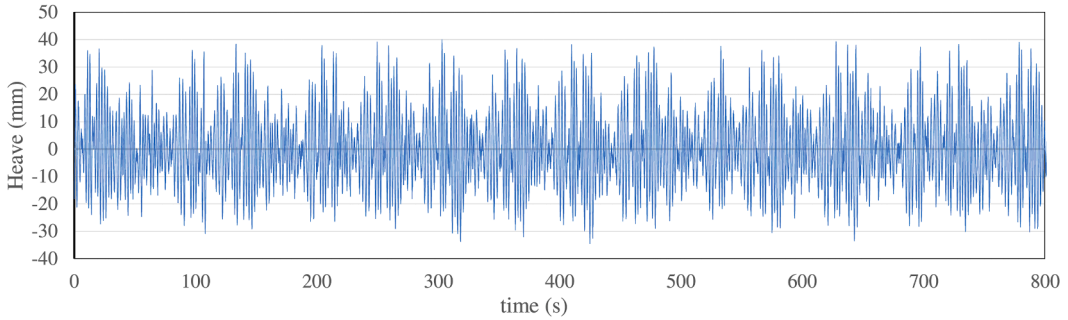

a)

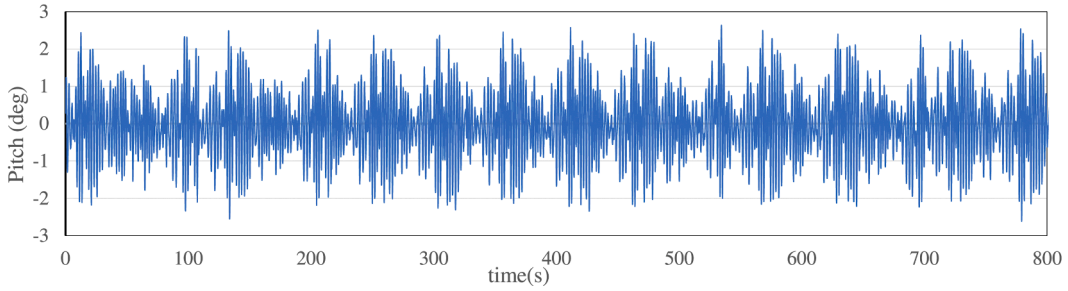

b)

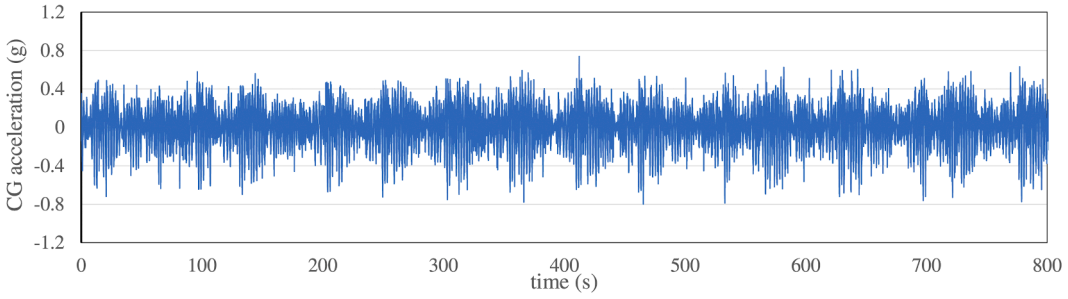

c)

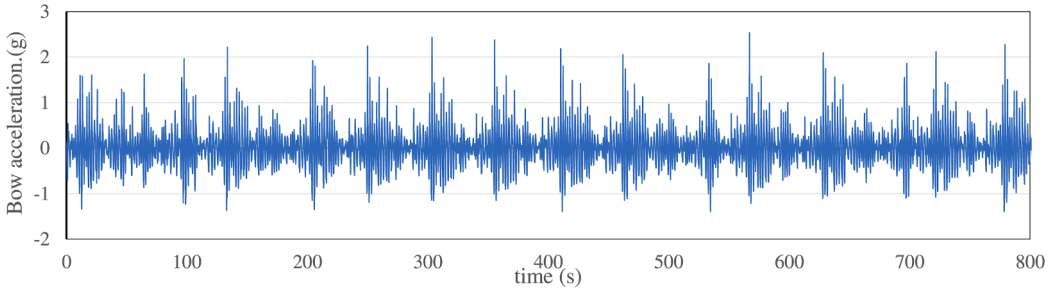

d)

Fig. A1. A time history of recorded a) heave, b) pitch, and vertical acceleration in c) CG and d) bow in wave condition 1 at $Fr_B = 2.2$.

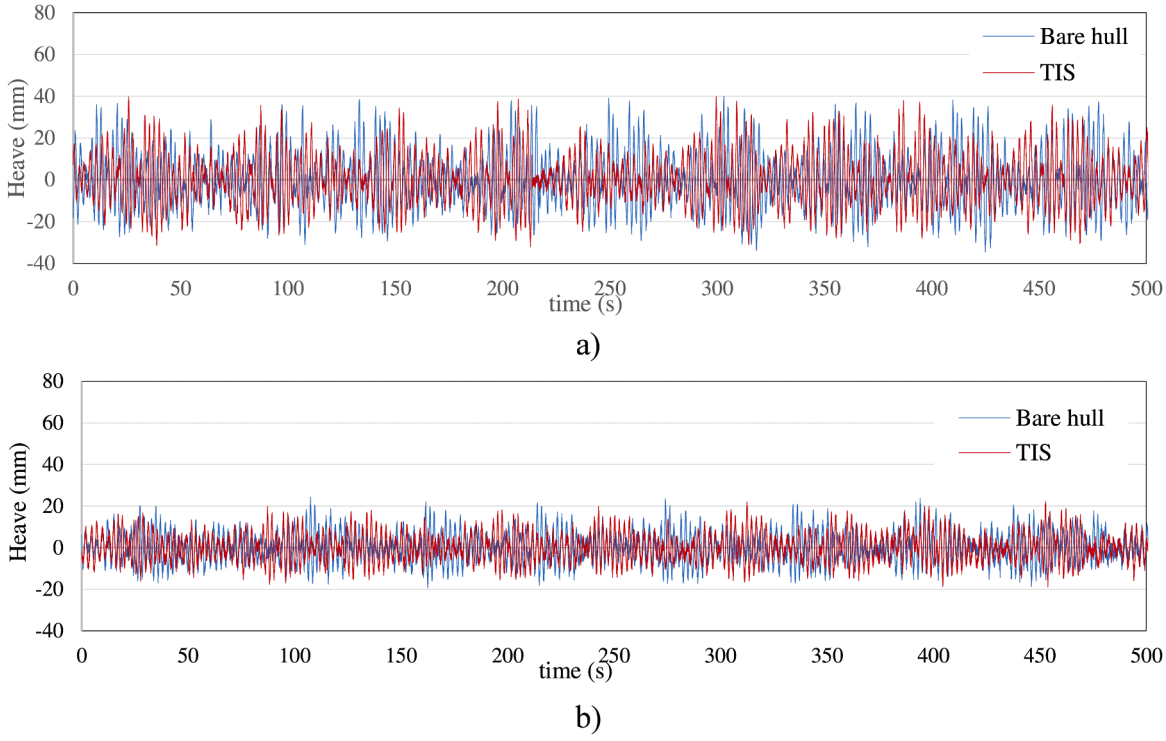

Fig. A2. Time history of heave motions for the bare hull and hull equipped with TIS in a) wave condition 1 and b) wave condition 2 at Fr_B=2.2.

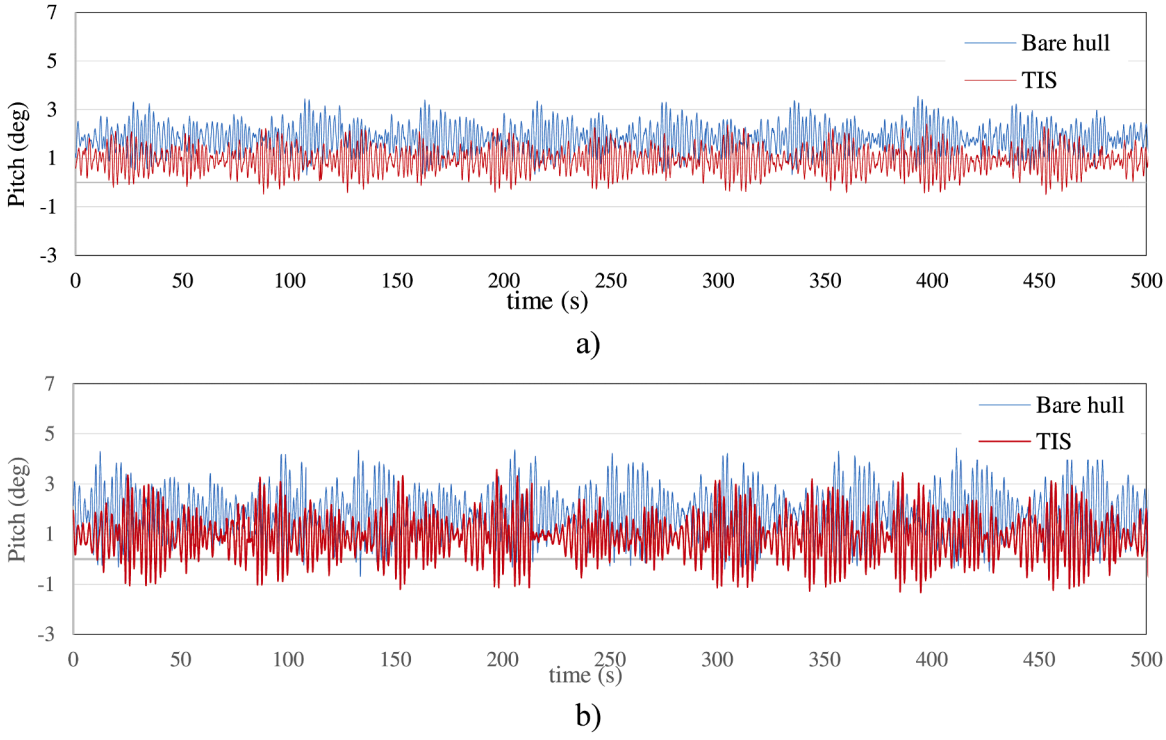

Fig. A3. Time history of pitch motion for the bare hull and hull equipped with TIS in a) wave condition 1 and b) wave condition 2 at Fr_B=2.2.

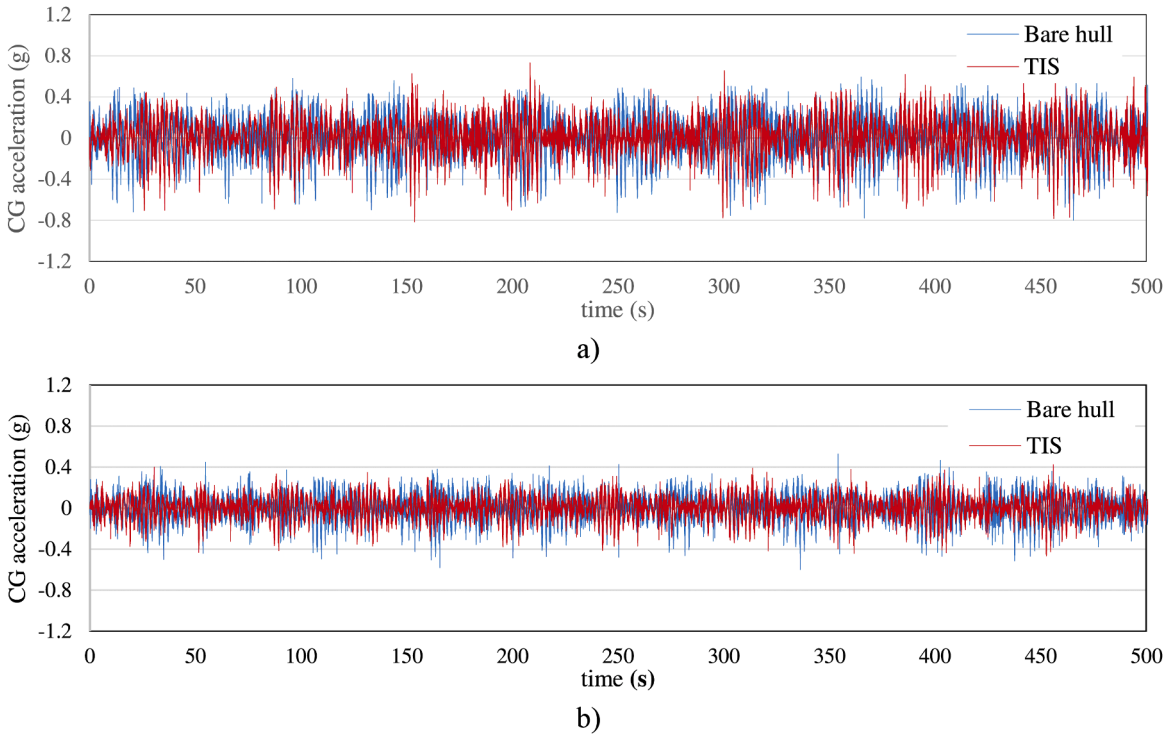

Fig. A4. Time history of the CG acceleration for the bare hull and hull equipped with TIS in a) wave condition 1 and b) wave condition 2, at Fr_B=2.2.

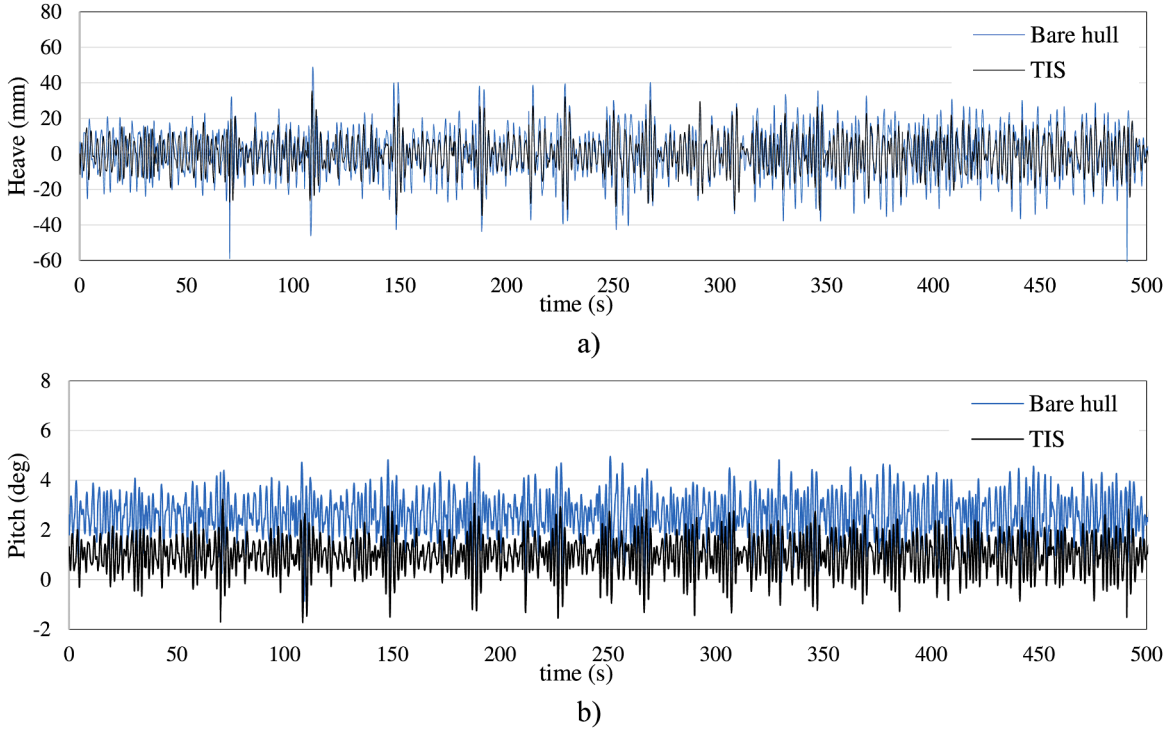

Fig. A5. TIS effect on a) heave and b) pitch motions in transient mode at Fr_B = 3.

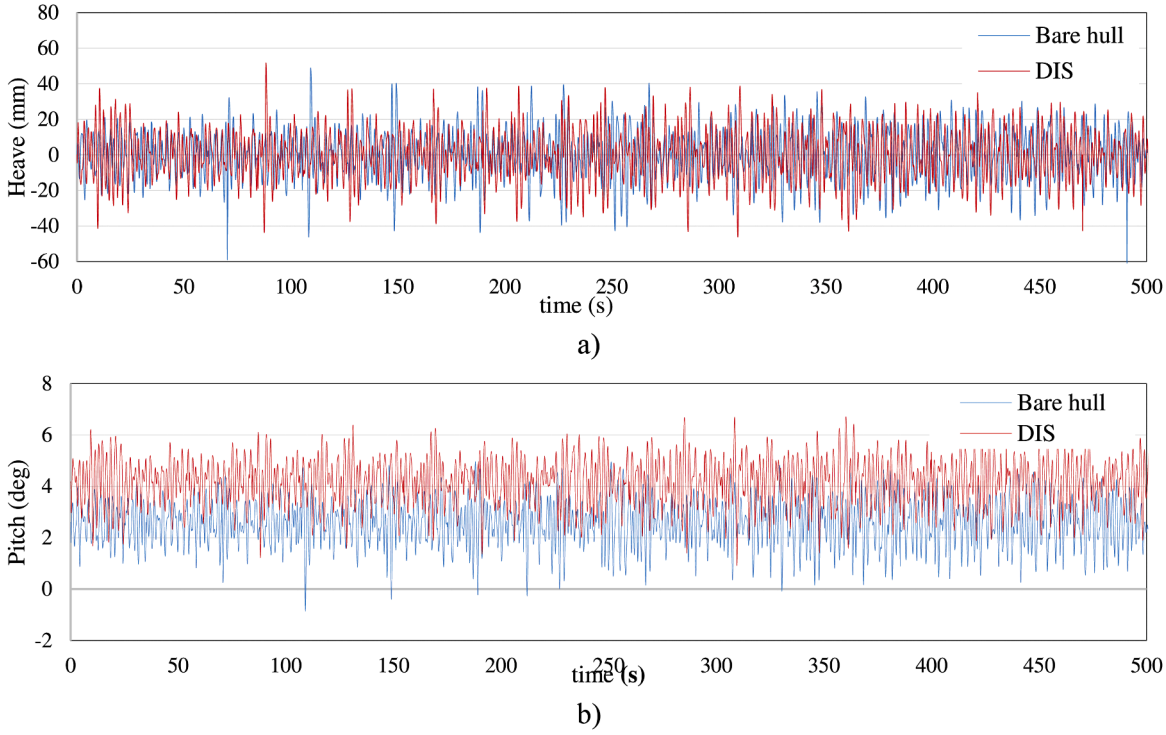

Fig. A6. DIS effect on a) heave and b) pitch motions in transient mode at $Fr_B = 3$.

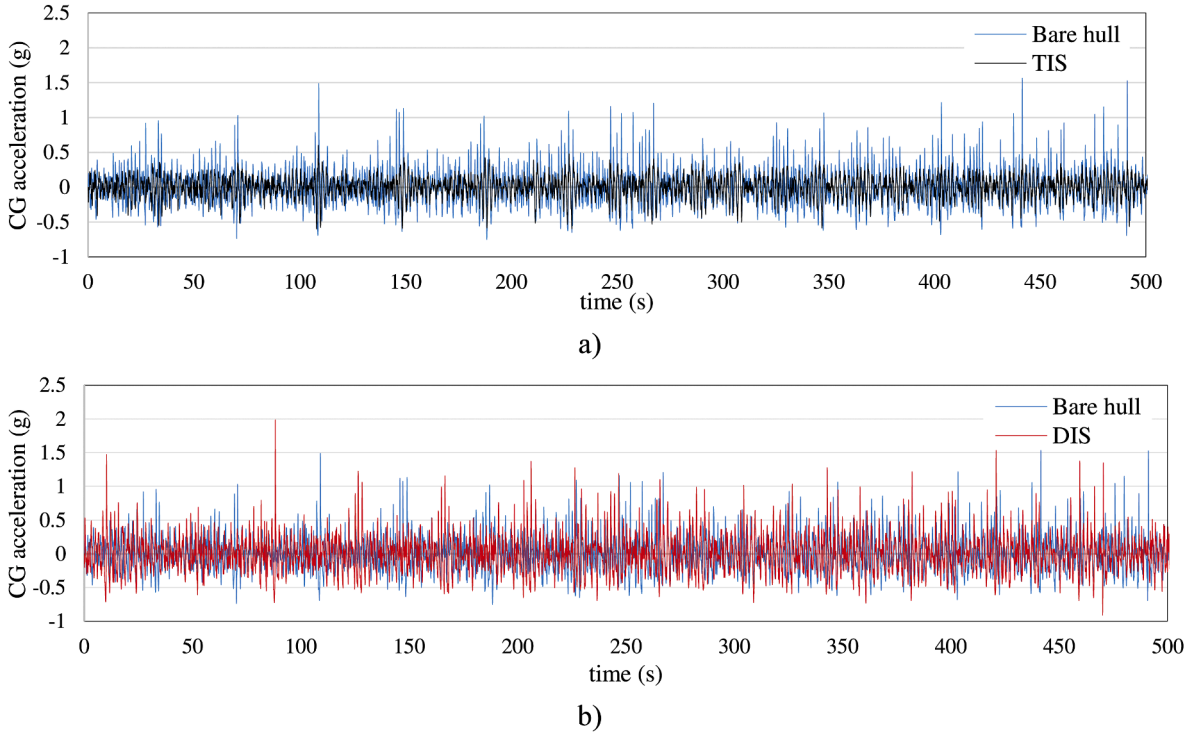

Fig. A7. Time history of CG acceleration in wave at $Fr_B = 3$ for a) bare hull and hull with TIS, and b) bare hull and hull with DIS.

References

ABCD Group. (2008). High Speed Craft Human Factors Engineering and Design Guide (ABCD TR-08-01 V1.0). Available online: https://www.ullmandynamics.com/wp-content/uploads/2011/02/hsc-human-factors-design-guide_2mg.pdf (accessed on 24 February 2022).

Allen, D.P., Taunton, D.J., Allen, R., 2008. A study of shock impacts and vibration dose values onboard highspeed marine craft. Trans. R. Inst. Naval Arch. Part A 150 (A3). Article A3.

Day, A.H., Cooper, C., 2011. An experimental study of interceptors for drag reduction on high-performance sailing yachts. Ocean Eng. 38 (8), 983–994. https://doi.org/10.1016/j.oceaneng.2011.03.006.

De Luca, F., Pensa, C., 2011. Experimental data on Interceptor's effectiveness. ITA. https://www.iris.unina.it/handle/11588/401517.
De Luca, F., Pensa, C., 2012. Experimental investigation on conventional and unconventional interceptors. Trans. R. Inst. Naval Arch. Part B 154, B65–B72. https://doi.org/10.3940/rina.ijsct.2012.b2.129.
De Luca, F., & Pensa, C. (2014). The prediction of the interceptor performances based on towing tank test data: ship-model correlation and hull form influence. 1, 231–238.
De Luca, F., Pensa, C., 2019. The Naples Systematic series – second part: irregular waves, seakeeping in head sea. Ocean Eng. 194, 106620. https://doi.org/10.1016/j.oceaneng.2019.106620.
De Luca, F., Pensa, C., 2017. The Naples warped hard chine hulls systematic series. Ocean Eng. 139, 205–236. https://doi.org/10.1016/j.oceaneng.2017.04.038.
Directive 2002/44/EC. (2002). Directive 2002/44/EC of the European Parliament and of the Council of 25thJune 2002on the Minimum Health and Safety Requirements Regarding the Exposure of Workers to the Risks Arising from Physical Agents (vibration).
Dobbins, T., Myers, S., Dyson, R., Withey, W., Gunston, T., & King, S., 2008. *High speed craft motion analysis: impact count index (ICI)*. 72. https://doi.org/10.3940/rina.surv.2009.09.
Garme, K., Burström, L., Kuttenkeuler, J., 2011. Measures of vibration exposure for a high-speed craft crew. *Proc. Inst. Mech. Eng.*, Part M 225 (4), 338–349. https://doi.org/10.1177/1475090211418747.
ISO 2631-1. (1997). *Mechanical vibration and shock—Evaluation of human exposure to whole-body vibration—Part 1: general requirements*. Int. Organ. Standardization, ISO, 2631-1. https://www.iso.org/standard/7612.html.
ISO 2631–5. (2004). *Shock–Evaluation of Human Exposure to Whole Body Vibration–Part 5: Method for Evaluation of Vibration Containing Multiple Shocks*. ISO: Geneva, Switzerland. https://www.iso.org/standard/7612.html.
John, S., Khan, M., Praveen, P., Korulla, M., & Panigrahi, P., 2011. Hydrodynamic performance enhancement using stern wedges, stern flaps and interceptors. Naval Science & Technological Laboratory, India.
Karimi, M.H., Seif, M.S., Abbaspoor, M., 2013. An experimental study of interceptor's effectiveness on hydrodynamic performance of high-speed planing crafts. Polish Maritime Res. 20 (2), 21–29. https://doi.org/10.2478/pomr-2013-0013.
Karimi, M.H., Seif, M.S., Abbaspoor, M., 2015. A study on vertical motions of high-speed planing boats with automatically controlled stern interceptors in calm water and head waves. Ships Offshore Struct. https://www.tandfonline.com/doi/full/10.1080/17445302.2013.867647.
Lau, C.-Y., Ali-Lavroff, J., Dashtimanesh, A., Holloway, D.S., Mehr, J.A., 2024. High-speed catamaran response with ride control system in regular waves by forcing function method in CFD. Ocean Eng. 297, 117111. https://doi.org/10.1016/j.oceaneng.2024.117111.
Mansoori, M., Fernandes, A.C., 2017. Interceptor and trim tab combination to prevent interceptor's unfit effects. Ocean Eng. 134, 140–156. https://doi.org/10.1016/j.oceaneng.2017.02.024.
Najafi, A., Alimirzazadeh, S., Seif, M.S., 2015. RANS simulation of interceptor effect on hydrodynamic coefficients of longitudinal equations of motion of planing catamarans. J. Braz. Soc. Mech. Sci. Eng. 37 (4), 1257–1275. https://doi.org/10.1007/s40430-014-0256-6.
Niazmand Bilandi, R., Tavakoli, S., Mancini, S., Dashtimanesh, A., 2024. Dynamic motion analysis of stepless and stepped planing hulls in random waves: a CFD model perspective. Appl. Ocean Res. 149, 104046. https://doi.org/10.1016/j.apor.2024.104046.
Park, J.Y., Choi, H., Lee, J., Choi, H., Woo, J., Kim, S., Kim, D.J., Kim, Kim, N., 2019. An experimental study on vertical motion control of a high-speed planing vessel using a controllable interceptor in waves. Ocean Eng. 173, 841–850. https://doi.org/10.1016/j.oceaneng.2019.01.019.
Putra, A.M.F., Suzuki, H., 2024. Experimental and numerical study on the high-speed ship hydrodynamics influenced by an interceptor with varied angle of attack. Int. J. Naval Arch. Ocean Eng. 16, 100566. https://doi.org/10.1016/j.ijnaoe.2023.100566.
Roshan, F., Dashtimanesh, A., Kujala, P., 2024. Safety improvements for high-speed planing craft occupants: a systematic review. J. Mar. Sci. Eng. 12 (5), 5. https://doi.org/10.3390/jmse12050845. Article.
Roshan, F., Tavakoli, S., Mancini, S., Dashtimanesh, A., 2022. Dynamic of tunneled planing hulls in waves. J. Mar. Sci. Eng. 10 (8), 8. https://doi.org/10.3390/jmse10081038. Article.
Seok, W., Park, S.Y., Rhee, S.H., 2020. An experimental study on the stern bottom pressure distribution of a high-speed planing vessel with and without interceptors. Int. J. Naval Arch. Ocean Eng. 12, 691–698. https://doi.org/10.1016/j.ijnaoe.2020.08.003.
Suneela, J., Krishnankutty, P., Subramanian, V.A., 2020. Numerical investigation on the hydrodynamic performance of high-speed planing hull with transom interceptor. Ships Offshore Struct. https://www.tandfonline.com/doi/full/10.1080/17445302.2020.1738134.
Suneela, J., Sahoo, P., 2021. Numerical investigation of interceptor effect on seakeeping behaviour of planing hull advancing in regular head waves. Brodogradnja 72 (2), 73–92. https://doi.org/10.21278/brod72205.
Taunton, D.J., Hudson, D.A., Shenoi, R.A., 2011. Characteristics of a series of high speed hard chine planing hulls - part II: performance in waves. Int. J. Small Craft Technol. 153, B1–B22. https://doi.org/10.3940/rina.ijsct.2011.b1.97.
Niazmand Bilandi, R. (2024). *Efficient high-speed small craft: performance in calm water and waves* [PhD degree, Tallinn University of Technology]. https://doi.org/10.23658/taltech.71/2024.
Tsai, F.J., Hwang, J.L., 2004. Study on the compound effects of interceptor with stern flap for two fast monohulls. In: IEEE Xplore Conference: MTTS/IEEE Techno-Ocean'04, Oceans'04, Taiwan, vol. 2. pp. 1023–1028 Nov. 9–12., doi:10.1109/OCEANS.2004.1405650.